

AEDC-TR-80-35

**ARCHIVE COPY
DO NOT LOAN**

c.1



Investigations of Free-Jet Test Requirements and Techniques with Emphasis on the Adaptable Jet Stretcher

R. J. Matz and E. M. Kraft
ARO Inc.

April 1981

Final Report for Period October 1, 1978 — September 30, 1979

**TECHNICAL REPORTS
FILE COPY**

Approved for public release; distribution unlimited.

PROPERTY OF U.S. AIR FORCE
AEDC TECHNICAL LIBRARY

Property of U.S. Air Force
AEDC TECHNICAL LIBRARY

AEDC TECHNICAL LIBRARY



5 0720 00034 6223

**ARNOLD ENGINEERING DEVELOPMENT CENTER
ARNOLD AIR FORCE STATION, TENNESSEE
AIR FORCE SYSTEMS COMMAND
UNITED STATES AIR FORCE**

NOTICES

When U. S. Government drawings, specifications, or other data are used for any purpose other than a definitely related Government procurement operation, the Government thereby incurs no responsibility nor any obligation whatsoever, and the fact that the Government may have formulated, furnished, or in any way supplied the said drawings, specifications, or other data, is not to be regarded by implication or otherwise, or in any manner licensing the holder or any other person or corporation, or conveying any rights or permission to manufacture, use, or sell any patented invention that may in any way be related thereto.

Qualified users may obtain copies of this report from the Defense Technical Information Center.

References to named commercial products in this report are not to be considered in any sense as an indorsement of the product by the United States Air Force or the Government.

APPROVAL STATEMENT

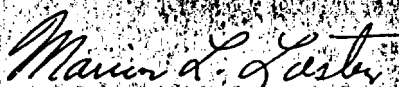
This report has been reviewed and approved



ROSS G. ROEPKE
Project Manager
Directorate of Technology

Approved for publication:

FOR THE COMMANDER



MARION L. LASTER
Director of Technology
Deputy for Operations

UNCLASSIFIED

DD FORM 1 JAN 73 1473 EDITION OF 1 NOV 65 IS OBSOLETE

UNCLASSIFIED

UNCLASSIFIED

20. ABSTRACT, Concluded.

Results obtained with subsonic and supersonic free-flight boundary conditions indicate that shortened forebodies can be used to reduce the overall length of test installations required for vehicles equipped with aft-mounted inlets. Bodies immersed in a supersonic free jet experience unacceptable flow distortions as a result of (1) bow shock reflections from the constant pressure free-jet boundary and (2) waves emanating from the nozzle lip because of exit plume static pressure mismatch. The adaptable jet stretcher can potentially eliminate these disturbances over a range of test conditions. A rigorous mathematical proof of jet stretcher convergence to the desired interference-free geometry was developed for supersonic flow. Convergence was also demonstrated by a computer experiment for a slender axisymmetric body in an off-design supersonic jet stretcher. Near field flow disturbances were reduced to an acceptable level after two readjustments of the jet stretcher geometry.

UNCLASSIFIED

PREFACE

The work reported herein was conducted by the Arnold Engineering Development Center (AEDC) of the Air Force Systems Command (AFSC). The results of the research were obtained by ARO, Inc., AEDC Group (a Sverdrup Corporation Company), operating contractor for the engine test facilities at AEDC, AFSC, Arnold Air Force Station, Tennessee, under Project Number E35A-01A. The authors gratefully acknowledge the assistance of W. J. Armstrong and G. W. Lewis, ARO, Inc., in the computational activities. The Air Force project manager was M. L. Laster. The manuscript was released for publication on May 28, 1980.

CONTENTS

	<u>Page</u>
1.0 INTRODUCTION	5
2.0 ANALYSIS	
2.1 Background	5
2.2 Free-Jet Test Requirements	9
2.3 Flow-Field Computations	10
2.4 Assessment of Jet Stretcher Feasibility and Implementation Problems	17
3.0 CONCLUDING REMARKS	19
REFERENCES	21

ILLUSTRATIONS

Figure

1. Flow-Field Characteristics about a Supersonic Vehicle with Different Boundary Conditions	23
2. Schematic of Near Field Streamline Patterns for a Cylinder in Crossflow with Various Boundary Conditions	27
3. Integration of the Test Cell and Computational Domain	28
4. Iterative Scheme for the Adaptable Jet Stretcher Concept	29
5. Details of Circular Arc Tangent/Ogive Bodies Used in Computations	30
6. Boundary Conditions and Computer Codes Used in the Flow-Field Computations	31
7. Flow Conditions Near a 1-cal Tangent/Ogive Body with Subsonic and Transonic Free-Flight Conditions	32
8. Flow Conditions Near a 2-cal Tangent/Ogive Body with Subsonic and Transonic Free-Flight Conditions	34
9. Flow Conditions Near a 3-cal Tangent/Ogive Body with Subsonic and Transonic Free-Flight Conditions	36
10. Flow Conditions Near a 2-cal Tangent/Ogive Body with Supersonic Free-Flight Conditions	38
11. Flow Conditions Near a 3-cal Tangent/Ogive Body with Supersonic Free-Flight Conditions	40
12. Comparison of Free-Jet Boundaries, Free-Flight Streamlines, and Cylindrical Duct Extensions Considered in the Subsonic Computations (3-cal Tangent/Ogive, $M_\infty = 0.6$)	42

<u>Figure</u>	<u>Page</u>
13. Flow Conditions Near a 3-cal Tangent/Ogive Body with $M_\infty = 0.6$ Free-Flight and Free-Jet Operation	43
14. Flow Conditions Near a 3-cal Tangent/Ogive Body with $M_\infty = 0.6$ Free-Flight and Ducted Operation	45
15. Comparison of Free-Jet and Free-Flight Flow Details (50-percent Blockage 3-cal Tangent/Ogive)	48
16. Flow-Field Details Produced by a 3-cal Tangent/Ogive Body in a Supersonic Free Jet	50
17. Comparison of Flow-Field Conditions Near a 3-cal Tangent/Ogive Body with Supersonic Free-Jet and Free-Flight Conditions	52
18. Extraneous Waves Introduced by Pressure Mismatch at Free-Jet Nozzle Exit	54
19. Streamline Trajectories at Various Supersonic Free-Flight Conditions about a 3-cal Tangent/Ogive Body	57
20. Computed Flow Conditions Near a 3-cal Tangent/Ogive Body with Iterative Jet Stretcher Adjustments	58
21. Characteristics Lines for Second Internal Iteration	62
22. Preliminary Thoughts on Possible Probe-Type Sensors for Perforated Adaptable Supersonic Jet Stretchers	63

TABLE

1. Current Free-Jet Design Goals	64
----------------------------------------	----

APPENDIX

A. Convergence of the Adaptable Jet Stretcher in Supersonic Flow	65
------------------------------------------------------------------------	----

NOMENCLATURE	72
--------------------	----

1.0 INTRODUCTION

Tests of full-scale engine/inlet systems in ground test facilities are limited at the present time because of the large air-processing systems required to achieve flow conditions representative of flight. Specially contoured ducts or “jet stretchers” have been proposed to reduce air supply requirements for engine/inlet tests in supersonic free-jet test facilities. However, fixed-geometry jet stretchers are unattractive because each test vehicle/test condition combination theoretically requires a different jet stretcher. Incorporation of variability — particularly in a feedback-controlled, online, adaptive mode — would greatly improve the potential usefulness of jet stretchers.

The objective of this study was to determine the requirements for, the alternatives to, and the feasibility of adaptable jet stretchers for both subsonic and supersonic free-jet testing. Feasibility was to be established in a rigorous mathematical sense and from representative flow-field computations for an axisymmetric body in free-flight, free-jet, and ducted flow environments. Results were also to be used to obtain a preliminary assessment of mechanical, instrumental, and computational requirements and to provide a basis for outlining additional work that must be accomplished before adaptable jet stretchers can become a practical test tool.

2.0 ANALYSIS

2.1 BACKGROUND

Problems arising from propulsion system integration in high-performance aircraft and missiles have plagued the aerospace industry for many years. Investigation of these problems with full-scale hardware has been hampered by the limited size and/or performance capabilities of ground test facilities. Some engine/inlet interaction tests have been conducted with full-scale air-breathing missile systems in free-jet test facilities of the AEDC Engine Test Facility (ETF). However, tests to date have been limited to relatively small vehicles having inlets located no more than two or three body diameters (or calibers) aft of the nose with simulated flight Mach numbers greater than two and angles of attack less than 10 deg. Under these conditions, it has been possible to locate the forward portion of the vehicle, including the inlet cowl, within the test rhombus of either planar, variable Mach number, or axisymmetric, fixed Mach number free-jet nozzles.

AEDC has received inquiries about supersonic, low-altitude tests of ramrocket-powered missiles with aft-mounted inlets (e.g., Fig. 1a) at angles of attack approaching 30 deg. A large wind tunnel (Fig. 1b) could provide the right Mach number, but the required

temperature and pressure conditions are beyond the capabilities of existing facilities. A smaller free-jet facility, capable of furnishing the desired temperature and pressure conditions, could be considered if extraneous effects such as the intersection of the bow shock with the constant pressure boundary (Fig. 1c) can be avoided or at least controlled to an acceptable degree. One scheme that has been proposed (Ref. 1) to effectively increase the length of the interference-free test rhombus is the so-called "jet stretcher" (Fig. 1d). A jet stretcher, which in reality is a "test rhombus stretcher," is a duct with an internal contour that corresponds to the portion of a streamline surface downstream of the bow shock generated by the vehicle being tested. The stretcher is positioned so that the flow within it is isolated from the bow shock interaction with the free boundary. Although the lip of the jet stretcher introduces a disturbance, careful design, fabrication, and alignment should produce flow conditions approaching the inlet that very closely approximate free flight.

Some theoretical and experimental investigations of axisymmetric jet stretchers, designed for use with axisymmetric test bodies, have been conducted (Refs. 2 through 5) to verify feasibility of the concept and to identify operational problems and performance constraints. Since the internal surface of the jet stretcher corresponds to a stream surface in the corresponding free-flight flow field about the test body, there is only one jet stretcher with a given inlet area that corresponds to a given set of test conditions (M_∞ , Re_∞^* , and attitude) for that test body. Some assessment of jet stretcher off-design performance, in terms of free-stream Mach number, axial location, and angular orientation with respect to the test body (Refs. 3 and 4) and porosity of the jet stretcher surface (Refs. 4 and 5), have been investigated as possible means of reducing cost and increasing flexibility of jet stretcher installations. Test body surface pressures obtained with free-stream Mach numbers that differed by 0.25 to 0.35 from design conditions were found to be acceptable. However, results obtained with angular mismatch and limited porosity in the jet stretcher are inconclusive based upon investigations to date. Furthermore, jet stretcher design and application has been limited to maximum angle-of-attack testing of about 5 to 10 deg where significant boundary-layer separation begins to occur (Ref. 6) on slender bodies. The relatively limited performance capability of a costly fixed-geometry jet stretcher, together with limitations of available analytical techniques required for design purposes, has significantly delayed development of the concept.

Continued concern about the interpretation of data obtained with wind tunnel models — particularly with transonic test conditions — has aroused interest in "self-correcting" or

*The internal jet stretcher contour is modified from a stream surface to account for boundary-layer development.

“adaptive wall” wind tunnels (Refs. 7 and 8). The basic problem, of course, is that the walls of a wind tunnel impose a boundary condition on the flow about a test vehicle (Fig. 2) that is not present in free flight. For example, a fixed, solid wall tunnel compresses the streamlines about a model (Fig. 2b) and artificially accelerates the local flow relative to conditions obtained in free flight (Fig. 2a) at the same initial Mach number condition. However, proper modification of the tunnel boundary condition by recontouring a solid wall tunnel (Fig. 2c) or by setting appropriate suction flows in a ventilated tunnel (Fig. 2d) will lead to streamline patterns and flow conditions that are comparable to free flight. The problem is the determination of the proper tunnel modification required, which is the objective of the adaptive wall test philosophy.

To understand how the adaptive wall concept might be applied to an adaptable jet stretcher, consider the flow situation created by an aerodynamic configuration in supersonic flight in a real fluid of unlimited extent (Fig. 3a). To simulate the flow field of Fig. 3 by a computational technique is difficult with the present state-of-the-art because of the complex geometry, strong viscous effects near the body, and shock-boundary layer interactions. Note, however, that the severe restrictions on the computational methods have to do with the region near the body. Computational methods can adequately simulate the conditions far from the body.

In contrast, if a test cell is considered as an analog computer, a good simulation of the flow near the body, which accurately accounts for the geometry and viscous interactions, can be provided. Unfortunately, because of the finite extent of the test cell it is difficult to simulate accurately the far field conditions (unless the test article is infinitesimally small).

Consequently, the ideal device to simulate the flow field of Fig. 3a would be a hybrid device using an analog simulator (the test cell) for the near field and a digital simulator (computational fluid dynamics) for the far field. The merging of the analog and digital devices can best be described by examining Fig. 3b where the infinite fluid region is divided into two parts, exterior (E) and interior (I) to an imaginary surface, S.

First, consider the flow in the exterior region. In the exterior region there are no immersed bodies; hence, viscous effects are essentially insignificant. Consequently, inviscid theories (such as the method of characteristics or, for small perturbations, linearized small-disturbance theory) which are well within the realm of practical computational methods can be applied in the exterior region. It is clear, then, at least in the inviscid approximation, the flow throughout the exterior region could be determined by prescribing the existing streamline slopes at S, for that would amount to prescribing the shape of the stream surface there. All other flow variables throughout the external region (and at S) are determined by these prescribed boundary values and the conditions at infinity. Hence, given the streamline

slopes at S , other variables such as the static pressure are uniquely determined by the strong conditions at infinity.

From the fact that the flow in the exterior region is determined by boundary values of a single variable at the surface, S , together with the conditions at infinity, it follows that two variables at S are adequate to define the conditions for unconfined flow. In other words, specification of two flow quantities all over S overdetermines the flow problem in the exterior region unless they have the required functional relationship with each other that satisfies unconfined flow at infinity.

Turning now to the interior region, note that the flow is determined by the stream parameters, the aerodynamic vehicle, and the values of the flow variables at S , without any approximations. Furthermore, if the interior region is replaced with a test cell with an adaptable jet stretcher (Fig. 3c), then to simulate the conditions of flight in that test cell, it is necessary and sufficient that conditions at S be the same as in unconfined flow (where S is any convenient surface within the cell). In general, these conditions are not met for an arbitrary jet stretcher configuration. If two flow quantities are measured at S , however, it could be ascertained by consideration of the boundary value problem in the region exterior to S if the measured flow quantities are consistent with the unconfined flow conditions at infinity. If they are not, then the jet stretcher geometry would have to be altered in some fashion to achieve unconfined flow conditions at the test article.

A basic iterative scheme of measurement and calculation for modifying the jet stretcher to achieve unconfined flow is shown in Fig. 4. For concreteness, the pressure distribution (P_I) and the flow angle relative to S (θ_I) are selected as the two flow variables measured at S . First, a flow field is established in the cell, and the flow variables, P_I and θ_I , are measured at the given control surface, S . The exterior unconfined region is then evaluated by specifying $\theta_E = \theta_I$ (subscript E designating the exterior region) as the boundary value at S . If the distribution at S of P_E determined from the exterior region calculations does not agree with P_I , the flow is still constrained by the jet stretcher and the jet stretcher must be readjusted. The iteration continues until P_I and P_E agree. The relaxation factor, k , is introduced to accelerate convergence of the iterative process.

The objective of the present work was to determine (1) requirements for and feasibility adaptable jet stretchers at AEDC, (2) compatibility with other free-jet hardware, and (3) additional work required for development of the concept. The method of approach included an assessment of currently envisioned free-jet test requirements at AEDC and an evaluation of alternate test techniques. A rigorous mathematical proof that the adaptive wall concept must converge to give free-flight conditions with supersonic flow was developed to

complement the proof previously developed (Ref. 9) for subsonic flow. Computations of inviscid perfect gas flow field conditions about simple axisymmetric shapes were used to determine differences between free-flight, free-jet, and ducted flow conditions. Computations were made for a test body and a mismatched jet stretcher to demonstrate convergence to supersonic free-flight conditions and to determine relative flow conditions at intermediate iterations. Implementation considerations and additional work required to ensure that the adaptable jet stretcher is, in fact, a practical test concept are also discussed.

2.2 FREE-JET TEST REQUIREMENTS

Current free-jet test activities at AEDC are limited to the ETF Aerodynamic and Propulsion Test Unit (APTU) where supersonic free-stream Mach number conditions in the range from 2 to 5 are achieved with fixed Mach number axisymmetric nozzles. Full-scale vehicles with cross-sectional areas (i.e., blockages) ranging from 5 to 50 percent of the nozzle exit area have been considered for test at preselected angles of attack up to 30 deg. In some proposed tests, the vehicle inlet is as much as 12 body diameters aft of the forebody nose. The APTU supersonic free-jet test approach assumes that only flow conditions in the theoretical nozzle test rhombus are acceptably representative of free-flight conditions. The forward portion of the vehicle to be tested, from the nose to the inlet cowl, must therefore be positioned within the test rhombus, and the APTU exhaust diffuser must be designed and operated to ensure that the free-jet nozzle is flowing full at all conditions of interest. Maximum angles of attack that can be achieved depend upon the free-jet nozzle design Mach number and size and the relative size and configuration of the test vehicle. Free-jet tests accomplished to date in APTU have been limited to maximum angles of attack of about 10 deg. No tests have been accomplished in APTU with jet stretchers.

Subsonic and supersonic free-jet test capabilities to be incorporated in the Aeropropulsion Systems Test Facility (ASTF) are currently under consideration. Presently perceived design goals (Table 1) include both steady-state and transient capabilities with both subsonic and supersonic flow and pitch and yaw variations. Tests of full-scale gas turbine engines, inlets, and any airframe surfaces that might affect flow approaching the inlets will require a large test rhombus since blockages, even at zero attitude conditions, will be in the 30- to 50-percent range. At maximum attitude angles, effective blockages will be even greater, and the flow process will be further complicated by impingement of the nozzle free-jet boundary on the test vehicle. Because of the limited extent of the free-jet nozzle test rhombus, it may not be possible to include all of the forward airframe components that might affect flow into the engine inlet. Under these conditions, an approximate shortened forebody will be used in conjunction with flow-field measurements in the vicinity of the initial inlet ramp. The forebody simulator and test conditions provided in ASTF will be

selected to produce flow conditions at some measurement station that are comparable to those obtained from preceding wind tunnel inlet model tests. Achieving the ASTF flow quality goals with all of the desired operational capability will be a formidable task.

2.3 FLOW-FIELD COMPUTATIONS

2.3.1 Approach

Computations of subsonic and supersonic flow fields around bodies representative of missile and aircraft forebodies were made to determine differences between free-flight, free-jet, and ducted flow conditions. Analysis was limited to axisymmetric bodies (Fig. 5) at zero angle of attack without inlet through-flow representation. Six different analytical models were employed since no single existing computer code has the demonstrated capability to handle this wide range of boundary conditions. Free-flight or infinite stream conditions (Fig. 6a) were obtained in the subsonic and transonic regimes with the South-Jameson finite-difference, relaxation solution of the full potential equation for axisymmetric inviscid flow (S-J, Ref. 10) while corresponding supersonic conditions were obtained with the Lockheed (LMOC, Ref. 11) and Armstrong three-dimensional (A3DMOC, Ref. 12) rotational method-of-characteristics codes. LMOC was used for the supersonic free jet (Fig. 6b) calculations and both LMOC and A3DMOC were used for the supersonic jet stretcher (Fig. 6c) evaluations. The time-dependent, finite-difference Cline nozzle and plume code (CNAP, Ref. 13) was the only analysis available for the subsonic free-jet (Fig. 6d) evaluations. Both CNAP and the Wehofer-Moger time-dependent, finite-difference analysis (W-M, Ref. 14) were used in the ducted subsonic flow (Fig. 6e) evaluations. The Douglas-Neumann panel method potential flow code (D-N, Ref. 15) was used to obtain subsonic infinite stream results (Fig. 6f) for comparison with CNAP and W-M results.

CNAP, because of its unique capability with the boundary conditions, had to be employed in the subsonic free-jet computations. However, considerable effort was necessary to achieve reasonably stable solutions representative of steady-state conditions. Various combinations of time step size and artificial viscosity factors were attempted with no apparent success within the 500 to 1,000 time steps (5 to 10 min CPU* time with 1,600 grid points) that were generally adequate for typical CNAP nozzle and plume computations. As a last resort, the nose of the forebody was modified on the premise that the differencing scheme used in CNAP has accuracy limitations which, in combination with the slope discontinuity at the forebody nose, might be aggravating the computational instabilities. The nose fairing was gradually increased in extent until reasonably stable flow conditions

*Computer times indicated are for the central processor unit (CPU) of an IBM 370/165 machine.

were achieved. This required a faired sting (Fig. 5) with cross-sectional area equal to 10 percent of the body. With this geometry and 8,000 time steps (95 min CPU time) stable, free-jet solutions were finally achieved* with a free-stream Mach number of 0.6. CNAP and W-M (55 min CPU time for 600 iterations with 21 by 111 grids) were used to evaluate the modified forebody in a cylindrical duct under subsonic conditions, and equivalent infinite stream results were obtained with D-N** (13 sec CPU time for 228 nodal points).

Unique capabilities and limitations of the A3DMOC and LMOC codes were weighed in the selection of the appropriate MOC analysis to use in a particular case. A3DMOC, because of its streamline tracking capability, was used to define supersonic jet stretcher geometries. The entropy "smearing" problem that occurs to some degree in all rotational MOC codes was noted in comparisons of near field flow properties (local total pressure and Mach number) obtained with A3DMOC and LMOC (CPU times = 11.3 and 1.3 min, respectively). Because of the reordering process necessary for the more general three-dimensional computations, entropy smearing is more severe in A3DMOC than in LMOC. For this reason and because of its general applicability to infinite stream, free-jet, and ducted boundary conditions, LMOC was used for the majority of the supersonic computations. AEDC modifications to the basic LMOC code provided plotting and interpolating capabilities and arbitrary pressure boundary input options that were both useful and necessary for manual iterations between internal and external adaptive jet stretcher conditions. Because of LMOC limitations, only body shapes and free-stream Mach numbers corresponding to attached bow shock conditions were considered in this study.

All of the computations made during this investigation were preliminary in nature since they are restricted to axisymmetric geometries and inviscid conditions. Flow fields associated with bodies and jet stretchers at angle of attack will be three-dimensional in nature with significant viscous effects near the surfaces which will, in extreme cases, lead to regions of separated flow. Furthermore, an inlet located at some point along the forebody, (Fig. 1a) will obviously alter the flow fields, as will the relative inlet capture/spillage conditions. However, theoretical investigations of the full viscous, compressible, three-dimensional problem this represents cannot be achieved until the appropriate algorithms are developed for this complex combination of boundary conditions.

*Computational instabilities increased as free-stream Mach number approached unity, even with the modified forebody.

**D-N, which includes a tangent gas approximation for compressibility effects, had to be used instead of the more precise S-J (3.3 min CPU time for a 97 by 97 grid) because S-J could not readily handle the modified forebody geometry. However, flow field computations made with both S-J and D-N for an unmodified 3-cal tangent/ogive and with D-N for the modified forebody with a Mach number of 0.6 yield substantially identical results within about four body radii from the unmodified nose station.

2.3.2 Infinite Stream Results

Forebody flow-field conditions experienced in an infinite stream were of interest for comparative purposes and for assessment of the potential for short forebody simulators. The ASTF flow quality goals (Table 1) were used as a criterion for determining adequacy of the test concept to represent free-flight conditions.

Body surface pressure coefficients and local free-stream Mach number and flow angle variations near the body surface where inlets would probably be located were determined for various caliber circular arc tangent ogives with subsonic, transonic, and supersonic flow conditions. The subsonic results (Figs. 7 through 9) indicate significant flow angle variations in the portion of the field near the body shoulder and for a distance corresponding to 1 to 2 body radii downstream. However, Mach number profiles indicate relatively uniform conditions even one body radius downstream of the tangent point on the one-caliber body (Fig. 7b). Therefore, for vehicles with forebodies like the circular arc tangent ogive with inlets located more than one body radius downstream of the shoulder, Mach number and flow angle variations should be uniform to well within the ASTF design goals of ± 0.05 on Mach number and ± 1 deg on flow angle if boundary-layer perturbations and/or separation are insignificant. Replacement of a longer forebody with a shorter version, therefore, appears to be a viable subsonic test approach at zero angle of attack if the test installation does not introduce significant extraneous effects such as shock/boundary interactions at supercritical flow conditions.

Infinite stream supersonic flow results (Figs. 10 and 11) indicate significant variations in flow angle, particularly near the body shoulder, and some Mach number variations that result from entropy gradients across the axisymmetric bow shock wave. However, downstream of the shoulder, particularly with free-stream Mach numbers less than 3, flow angle and Mach number variations are uniform to within the ± 0.6 deg and ± 0.05 Mach number ASTF design goals. Therefore, use of a shortened forebody also appears to be a viable option at supersonic test conditions.

2.3.3 Subsonic Free-Jet Results

The major concern in all wind tunnel and free-jet tests is that the test section or free-jet boundary will impress or reflect extraneous flow conditions on the test body that are not representative of free flight. This was investigated with a limited series of computations involving the modified 3-cal tangent ogive in free jets corresponding to 10- and 50-percent blockage conditions. Because of the computational stability problems with CNAP, only one subcritical free-stream condition corresponding to 0.6 Mach number could be considered during the time period of this study.

The constant pressure free-jet boundaries corresponding to both the 10- and 50 percent blockage configurations were found to very closely approximate the infinite stream 10- and 50-percent streamlines for the case considered (Fig. 12). The constant pressure free-jet boundary alters body pressure distributions upstream of the shoulder region to some degree (Fig. 13a) and apparently causes a more rapid return to free-stream conditions downstream of the shoulder than occurs under infinite stream conditions. Local free-stream Mach numbers and flow angles (Fig. 13b) are within ± 0.01 and ± 0.5 deg, respectively, of infinite stream conditions even on the contoured portion of the modified forebody where the most significant variations occur in body surface pressure coefficients. Although these results indicate surprisingly good agreement between free-jet and infinite stream conditions even with substantial blockages, care must be exercised to avoid sweeping conclusions about relative subsonic free-jet flow conditions based upon this single set of idealized (modified forebody with inviscid, subcritical, zero angle-of-attack conditions) results without additional theoretical or experimental confirmation.

2.3.4 Subsonic Jet Stretcher Consideration

One of the planned work items of this study was to accomplish a series of iterative computations to demonstrate that flow conditions about a body do, in fact, relax to free-stream conditions with an adaptable subsonic jet stretcher. Cylindrical extensions (Fig. 12) of the free-jet nozzle were selected as an initial geometry for the jet stretcher, and computations were initiated with CNAP. Although the CNAP computational instability problems precluded completion, the available results do offer some information for consideration. For example, choking considerations limit subsonic Mach numbers upstream of a 50-percent blockage model in a cylindrical duct to something less than 0.3. With this constraint it might be concluded that representative flow conditions for a free-flight Mach number of 0.6 could not be achieved. This would indeed be true if comparable high quality (i.e., wind tunnel) flow conditions were required *over the entire body*. However, in the proposed ASTF free-jet test philosophy, representative flow conditions will only be required in the vicinity of the induction system inlet. With this concession, it should be possible to select test conditions (i.e., overall pressure ratio and/or jet stretcher geometry) to produce desired nominal levels and distributions of Mach number and flow angle at the induction system inlet even though there are significant mismatches in other regions of the flow field. This is illustrated most dramatically by the CNAP results for a modified 3-cal tangent ogive in a cylindrical duct.

Because of the choking problem and the CNAP input requirements, the ducted subsonic computations were made with the duct exit Mach number set at 0.6. Pressure coefficients (Figs. 14a and b, based on $M = 0.6$ at $X/R_o = 16$) indicate the significant overall fore-to-aft deviations from free flight that can be expected with significant blockages on both the

model and the outer boundary. However, with matched downstream conditions, the major differences between free flight and ducted flow are forced to occur near the upstream end of the test body. Even for the extreme case represented by the 50-percent blockage model in a cylindrical duct, computed flow conditions at the shoulder ($X/R_o = 6$) agree with free flight to within 0.03 on Mach number and 0.5 deg on flow angle (Fig. 14c). Four body diameters ($X/R_o = 8$) downstream of the nose station, all computed results (free flight, ducted, and free jet) were found to agree within ± 0.01 on local Mach number and ± 0.3 deg on local flow angle. Since the radial distributions are similar in shape, it appears that the agreement between ducted, free-jet, and free-flight results could be further improved if necessary with only slight adjustments in boundary conditions. Although these results are probably representative for any slender body of interest with subcritical flow, additional investigations are required to determine if they are significantly altered when supercritical conditions occur.

2.3.5 Supersonic Free-Jet Results

The principal cause for differences between supersonic free-flight and free-jet flow conditions is the reflection of body-generated compression and rarefaction waves which significantly alter the constant pressure free boundary shape from the corresponding free-flight streamline (Fig. 15). The reflected rarefaction zone from the bow shock/free boundary interaction (Fig. 16a) and subsequent reflections from the body and free boundary (Fig. 16b) can significantly alter near field conditions (Fig. 17), particularly when high blockage bodies are evaluated at low supersonic Mach numbers.

Any mismatch between free-jet boundary (i.e., test cell) and free-jet nozzle lip pressure also introduces extraneous waves that can distort supersonic free-jet test results. An expansion fan (Fig. 18a) or a compression wave (Fig. 18b) will emanate from the free jet nozzle lip depending upon the relative magnitudes of the nozzle lip and jet boundary pressures. These waves will impinge upon and reflect from the test body in a manner that could—with a significant pressure mismatch—unacceptably distort the flow (Fig. 18c) entering an aft-mounted inlet.

2.3.6 Supersonic Jet Stretcher Results

A properly designed jet stretcher can minimize the effect of bow shock interactions with a free-jet boundary. Also, if the jet stretcher lip size and location are properly selected, the flow field of interest can be isolated (Fig. 1d) from extraneous waves produced by mismatches between the nozzle lip and test cell pressures. However, a fixed-geometry jet stretcher has obvious limitations as indicated by a comparison of free-flight streamline

trajectories (Fig. 19). Even with a particular body and blockage combination and allowance for differences in the bow shock location, free-stream Mach number alters the downstream streamline shape that a jet stretcher must assume. Considering the additional requirements for angle-of-attack testing with a variety of vehicle geometries, the need for variability, preferably with rapid, online feedback control, is almost a necessity to ensure practicability of the jet stretcher concept.

A major concern in the adaptable jet stretcher philosophy is that convergence to free-flight conditions can indeed be obtained from some arbitrary initial condition in a reasonable number of iterations. For this reason previous mathematical proofs of the convergence of transonic adaptive wall wind tunnels to unconfined or infinite stream conditions (Ref. 9) were extended to supersonic flow and are included in the Appendix. Convergence was further demonstrated in a series of computations where the interior flow field conditions between a typical body and an off-design jet stretcher, which would normally be obtained in a test installation, were computed with LMOC. The corresponding exterior region computations, which would normally be made online in an actual adaptive test mode situation, were also accomplished with LMOC.

A 3-cal tangent/ogive was evaluated in a Mach number 2.3 airstream with an off-design jet stretcher configuration corresponding to an axially shifted, 50-percent blockage Mach number 5.0 streamline. Body surface pressure coefficients (Fig. 20a) and near field flow conditions (Figs. 20b and c) obtained with the shifted, mismatched jet stretcher indicate significant deviations from infinite stream conditions, largely because of the 1.9-deg mismatch (Fig. 20d) at the jet stretcher lip.

From the initial mismatched flow condition, the jet stretcher contour was varied through a series of exterior/interior region iterations until near field Mach numbers and flow angles agreed with infinite stream results to within ± 0.05 on Mach number and ± 0.6 deg on flow angle. Streamwise distributions of static pressure near the jet stretcher surface were used to define the outer boundary conditions for the interior region computations. The resulting outer boundary streamline contours, computed from the interior solutions, were then used as a boundary condition in the exterior region computations. Typical LMOC CPU times were 20 and 50 sec, respectively, for the interior and exterior computations. LMOC had to be modified to accept streamwise variations of pressure as a function of axial position and to accomplish spline fits which could be used in the interior computations.

The sequence of events in the iterations was as follows:

1. Interior flow-field conditions were obtained with the off-design jet stretcher contour as the outer boundary to establish initial pressure distributions $[P_I^0(X)]$ along the jet stretcher surface with $M_\infty = 2.3$.
2. An initial exterior region computation was made with a hypothetical axisymmetric body, having the off-design jet stretcher contour, in an infinite $M_\infty = 2.3$ stream to define surface pressure distributions $[P_E^0(X)]$.
3. The initial exterior and interior pressure distributions were compared and a first iteration internal pressure distribution $[P_I^1(X)]$ was established from

$$P_I^1(X) = k \left[P_I^0(X) \right] + (1 - k) \left[P_E^0(X) \right]$$

where k , the weighting factor, was arbitrarily set at 0.5.

4. A first iteration internal solution was accomplished with a varying pressure outer boundary represented by $P_I^1(X)$ to determine the first iteration jet boundary shape.
5. A first iteration exterior solution was accomplished with a hypothetical axisymmetric shape corresponding to the first iteration jet boundary contour to determine the corresponding surface pressure distribution.
6. $P_I^1(X)$ and $P_E^1(X)$ were used to establish a second iteration pressure distribution from

$$P_I^2(X) = k \left[P_I^1(X) \right] + (1 - k) \left[P_E^1(X) \right]$$

7. A second iteration internal solution was accomplished with $P_I^1(X)$ as the outer boundary.

Changes in body surface pressure coefficients and near field Mach number, static pressure, and flow angle for the two iterations are shown in Fig. 20. Although all parameters indicate a general convergence to infinite stream conditions, there is still evidence (Figs. 20d and 21) of some residual mismatched conditions near the jet stretcher lip that are being reflected downstream after the second iteration. This mismatch is attributed in part to the upstream boundary conditions used in the interior computations and could probably be eliminated with a more careful selection of LMOC starting line point conditions. Secondary ripples in the body surface pressure coefficients, particularly with the initial off-design jet

stretcher geometry, are probably indicative of irregularities in the jet stretcher contour that are produced by the combination of the number of points selected and the resulting spline fits.

2.4 ASSESSMENT OF JET STRETCHER FEASIBILITY AND IMPLEMENTATION PROBLEMS

2.4.1 General Remarks

Although actual evaluation of the adaptable jet stretcher concept was very limited and confined to the relatively simple case represented by an axisymmetric body at zero angle-of-attack in axisymmetric supersonic and subcritical, subsonic inviscid jets, the results obtained do indicate feasibility of the approach. However, there is obviously a large step from the limited feasibility demonstrated in this study to the provision of a practical system that can be used in either APTU or ASTF. Further investigations, both theoretical and experimental, are obviously required. Three-dimensional subsonic and supersonic computational capability for general bodies embedded in planar or axisymmetric flow fields is required to extend the feasibility studies to relevant ASTF and APTU test considerations. Some experimental model studies will also be required to evaluate control systems, instrumentation concepts, and external region computational algorithms. When an appropriate computer code becomes available, relative effects of flow into the engine inlet on jet stretcher aspects should also be considered, particularly with subcritical inlet operation.

High angle-of-attack tests of large bodies that will penetrate a subsonic free-jet boundary will create unique flow problems that may be difficult to correct with a jet stretcher. After the planned FY 81/82 ASTF subsonic free-jet model tests in Propulsion Research Cell (R-2A2) are accomplished, a better assessment can be made about the potential role of adaptable jet stretchers in subsonic free-jet testing.

High angle-of-attack testing of slender vehicles with aft-mounted engine inlets could also be difficult to handle with jet stretchers. Extension to angles of attack up to about 20 deg, where separation occurs on the vehicle in a fairly simple, time-wise steady manner (Ref. 6), may be possible. However, the asymmetric shedding of multiple vortex sheets observed (Ref. 6) with slender vehicles at higher angles of attack will pose even more formidable implementation problems.

Incorporation of adaptable jet stretchers in APTU will require a high-response control system and a fast external flow algorithm that are compatible with the limited blowdown

times. Incorporation into ASTF will depend to a large degree on compatibility with the planar free-jet nozzle and associated free-jet spillage diffuser systems actually used.

2.4.2 Jet Stretcher Control

In actual tests, the two independent flow parameters required for the jet stretcher adjustments must be measured along some reference surface (or surfaces) in the vicinity of the jet stretcher surface. Ideal measurable flow parameters for this purpose would be (1) simple to obtain, (2) noninterfering, and (3) highly responsive to jet stretcher adjustments. In current subsonic/transonic adaptive wind tunnel wall studies, flow-field measurements made depend upon the manner in which the effective wall shape is achieved. If a flexible wall is employed (Ref. 8), wall static pressure distribution and contour geometry are the control parameters. In a perforated or slotted tunnel (Ref. 7), where effective outer boundary shape is changed by air injection or removal, static pressures and flow angles are usually measured with static pressure pipes and hemisphere/cylinder probes at some reference surface near the wall but outside the boundary-layer interaction region. Static pressure measurements from two different reference surfaces are also being considered as an alternative. Comparable measurements could be made in a subsonic jet stretcher.

Actually recontouring the wall of a jet stretcher required for three-dimensional supersonic flow with temperatures greater than 200 to 300°F will be extremely difficult. If effective shaping is accomplished with air injection or removal, control parameter measurements are more of a problem. Optical techniques, such as laser velocimeters, would pose formidable installation and operational problems. On the other hand, insertion of probes into the supersonic airstream will introduce extraneous compression and expansion waves. Calibrated cone probes or double wedge airfoil sections (Fig. 22) extending beyond the interaction zone might be used for supersonic adjustable jet stretcher control parameter measurement if the extraneous waves can be tolerated. In any case, the probes must be carefully designed to be as small as possible and to extend no farther beyond the boundary-layer/inbleed interaction zone than necessary. Careful consideration must also be given to the number and placement of the probes to ensure that measurements are obtained at the most critical regions with a total number of parameters that can be accommodated by the available data acquisition and conditioning equipment.

2.4.3 Online Exterior Flow Computations

The present studies indicate that the method of characteristics is a reasonable algorithm to use, at least for axisymmetric flow, in the online exterior flow computations for supersonic flow. A new computer code must be formulated to take the specified measured

quantities, make the appropriate characteristics computations, assess the adequacy of current conditions, and then provide an output that can be converted into an appropriate signal to inbleed/outbleed control valves. The relatively high computational speeds achieved with a general program like LMOC suggest that CPU time should not be a problem for a tailored MOC code. However, the code should be constructed with time optimization in mind since this may be crucial to satisfactory operation with a blowdown facility like APTU.

The subsonic/transonic free-flight results presented herein suggest that elements of the potential flow and finite-difference algorithms incorporated in D-N and S-J could be employed for external region computations with subsonic adaptable jet stretchers. The potential flow option is particularly attractive because of its flexibility and speed; however, it is limited to subsonic conditions on the reference surface. Algorithms being developed for adaptive transonic wind tunnel applications should also be considered for extension to subsonic jet stretchers. For example, the Prandtl-Glauert form of the linear small disturbance equations and a finite-difference formulation of the transonic small disturbance equation have been used (Ref. 16), respectively, with subsonic and transonic flow conditions at the reference surface. Further investigations are required to determine advantages and disadvantages of extending these and other adaptive wind tunnel external flow analyses to subsonic/transonic jet stretchers.

3.0 CONCLUDING REMARKS

Approaches that will permit relatively large airbreathing engine/inlet/forebody systems to be free-jet tested in APTU and ASTF received preliminary investigation. Conclusions were based upon near field flow properties (Mach number and flow angle) obtained from inviscid flow computations for slender, axisymmetric bodies at zero incidence using ASTF flow quality design goals as an acceptance criterion.

Results obtained with subsonic and supersonic free flight boundary conditions indicate that shortened forebodies can be used to reduce the overall length of test installations required for vehicles equipped with aft-mounted inlets.

Limited axisymmetric calculations for slender bodies immersed in free jets at subcritical flow conditions indicate streamlines and local steady-state flow properties that are comparable to free-flight conditions to well within the ASTF flow quality goals. However, this agreement is favorably biased in the calculations by an artificial upstream extension to the forebody which was necessary to reduce computational instabilities. Although the instability problems precluded quantitative verification that an adaptable jet stretcher could reduce differences between subsonic free-jet and free-flight results, the ongoing transonic

wind tunnel adaptive wall studies and the limited results obtained on this study do tend to support this premise.

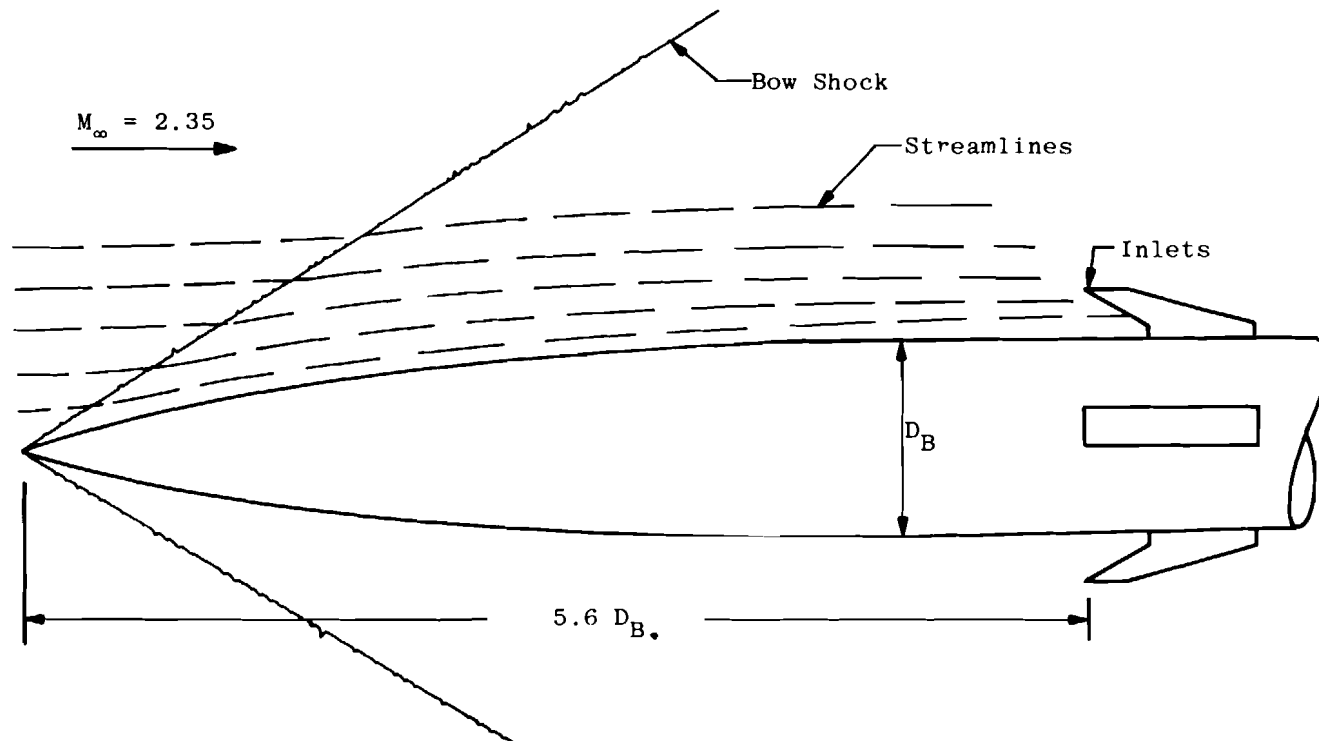
Bodies immersed in a supersonic free jet experience unacceptable flow distortions as a result of (1) bow shock reflections from the constant pressure free-jet boundary and (2) waves emanating from the nozzle lip because of exit plume static pressure mismatch. The adaptable jet stretcher can potentially eliminate these disturbances over a range of test conditions. A rigorous mathematical proof of jet stretcher convergence to the desired interference-free geometry was developed for supersonic flow to complement the previously developed proof for subsonic conditions. Convergence was confirmed by a computer experiment for a slender axisymmetric body in an off-design supersonic jet stretcher. Near field flow disturbances were reduced to an acceptable level after two readjustments of the jet stretcher geometry.

The method of characteristics appears to be an acceptable algorithm for external region calculations with supersonic adaptable jet stretchers. Adaptation of linear small disturbance and finite-difference formulations under development for adaptive transonic wind tunnels should be possible for external flow computations in subsonic jet stretchers.

REFERENCES

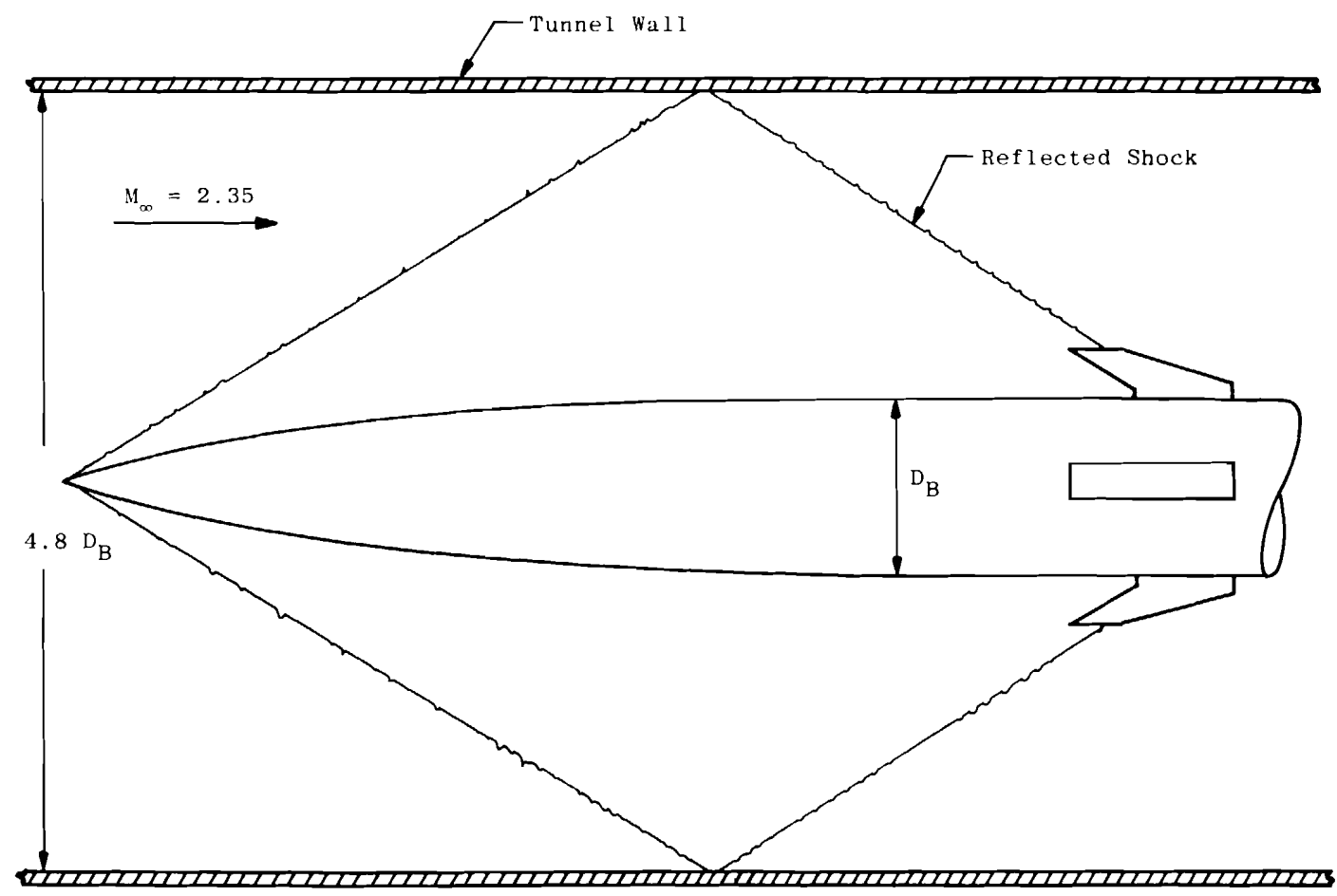
1. Himmler, E. B., et al. "A Special Technique for Free-Jet Testing of Aft-Inlet Systems." The Marquardt Corporation Report MP-1429, November 1966.
2. German, R. C. "Simulation of Supersonic Flow Over a Body of Revolution Using an Axisymmetric Jet Stretcher." AEDC-TR-70-166 (AD875834), October 1970.
3. Barebo, R. L. and Matkins, E. H. "Simulation of Supersonic Flow Over a Scale Model Missile with Aft-Mounted Inlets Using an Axisymmetric Jet Stretcher." AEDC-TR-71-37 (AD514891), April 1971.
4. Eppright, B. R. "Theoretical Effects of Porosity and Angle-of-Attack on Jet Stretcher Performance." University of Texas, PhD Dissertation, May 1971.
5. Bauer, R. C. et al. "A Theoretical and Experimental Study of a Jet Stretcher System." *Journal of Spacecraft and Rockets*, Vol. 10, No. 6, June 1973, pp. 395-405.
6. Przirembel, C. E. A. and Shereda, D. E. "Aerodynamics of Slender Bodies at High Angles of Attack." *Journal of Spacecraft and Rockets*, Vol. 16, No. 1, January-February 1979, pp. 10-14.
7. Sears, W. R. "Self Correcting Wind Tunnels." *Aeronautical Journal*, Vol. 78, No. 758-759, February-March 1974, pp. 80-89.
8. Goodyer, M. J. "The Self-Streamlining Wind Tunnel." NASA Langley Research Center Report NASA TMX-72699, August 1975.
9. Lo, C. F. and Kraft, E. M. "Convergence of the Adaptive Wall Wind Tunnel." *American Institute of Aeronautics and Astronautics Journal*, No. 1, January 1978, pp. 67-72.
10. South, J. C., Jr. and Jameson, A. "Relaxation Solutions for Inviscid Axisymmetric Transonic Flow over Blunt or Pointed Bodies." Proceedings of the First AIAA Computational Fluid Dynamics Conference, Palm Springs, California, July 19-20, 1973.
11. Smith, S. D. and Ratliff, A. W. "Rocket Exhaust Plume Computer Program Improvement, Vol. IV." Lockheed Missiles and Space Company Report LMSC/HREC D162220-IV-A, June 1971.
12. Armstrong, W. C. and Bauer, R. C. "Analysis of Three-Dimensional Inviscid Supersonic Flow Between a Body and an Outer wall (with Application to a Jet Stretcher System)." AEDC-TR-76-103 (AD-A029123), August 1976.

13. Cline, M. C. "NAP: A Computer Program for the Computation of Two-Dimensional, Time-Dependent, Inviscid Nozzle Flow." Los Alamos Scientific Laboratory Report LA-5984, January 1977.
14. Wehofer, S. and Moger, W. C. "Analysis and Computer Program for Evaluation of Airbreathing Propulsion Exhaust Nozzle Performance." AEDC-TR-73-29 (AD760541), May 1973.
15. Hess, J. S. and Smith, A. M. O. "Calculation of Potential Flow About Arbitrary Bodies." *Progress in Aeronautical Sciences*, Vol. 8, Pergamon Press, New York, 1967.
16. Kraft, E. M. and Parker, R. L., Jr. "Experiments for the Reduction of Wind Tunnel Wall Interference by Adaptive-Wall Technology." AEDC-TR-79-51 (AD-A076555), October 1979.

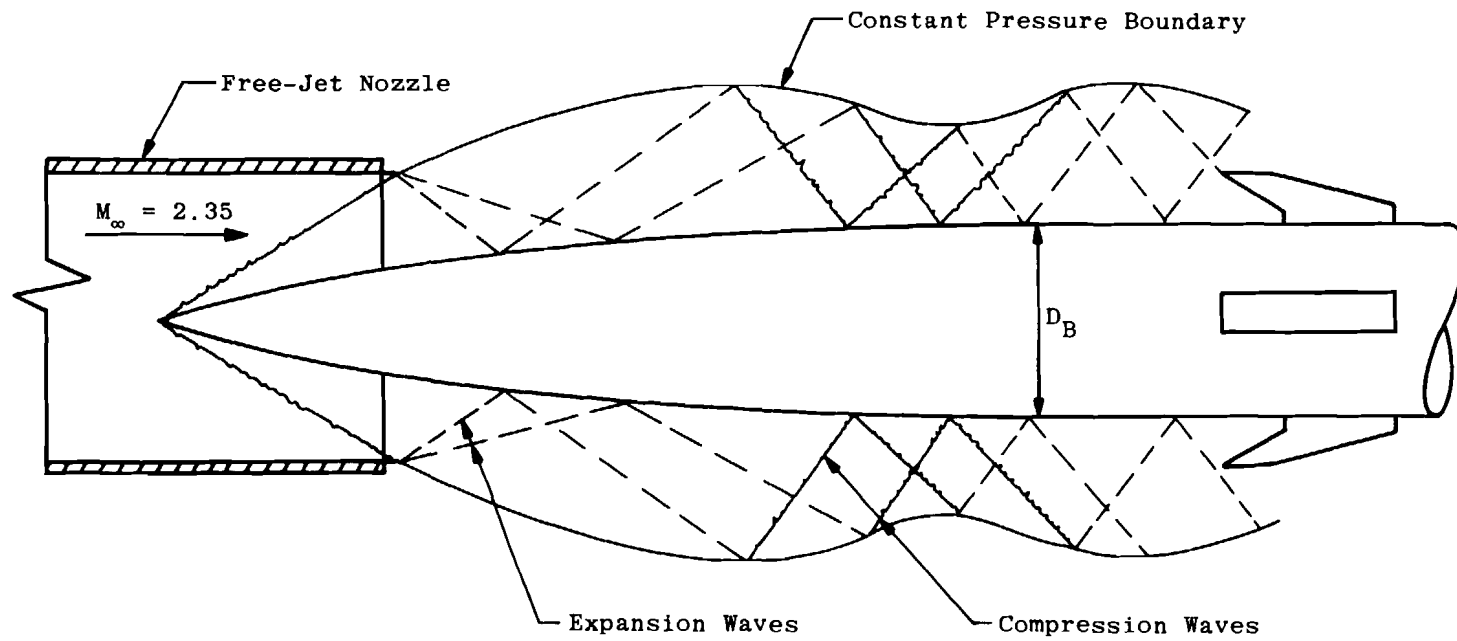


a. Free flight

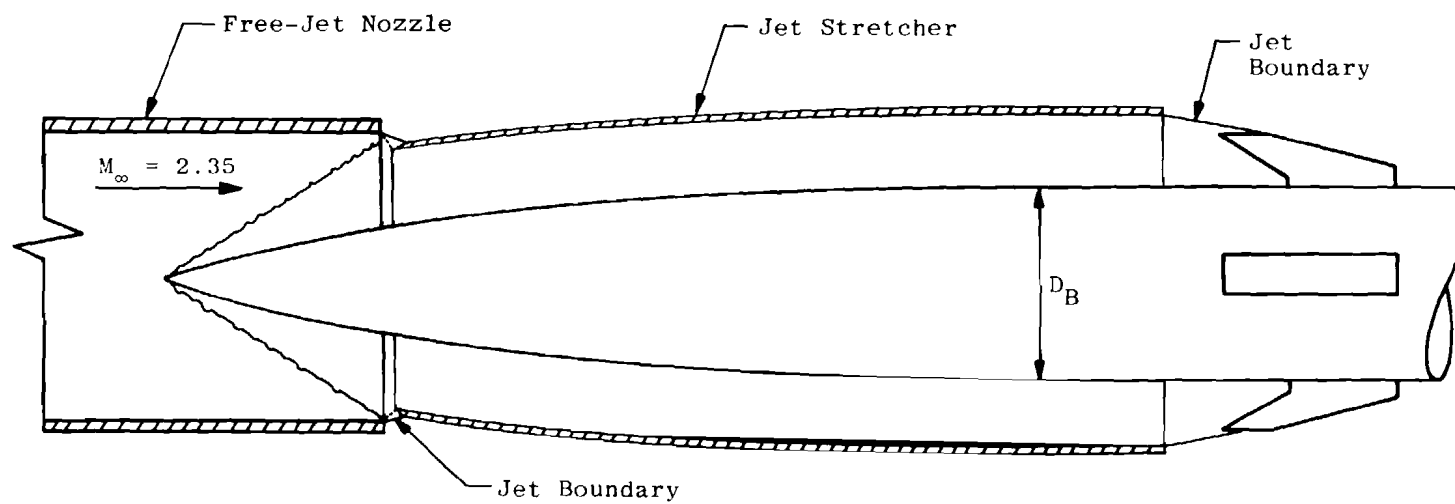
Figure 1. Flow-field characteristics about a supersonic vehicle with different boundary conditions.



b. Wind tunnel
Figure 1. Continued.



c. Free jet
Figure 1. Continued.



d. Free jet with jet stretcher
Figure 1. Concluded.

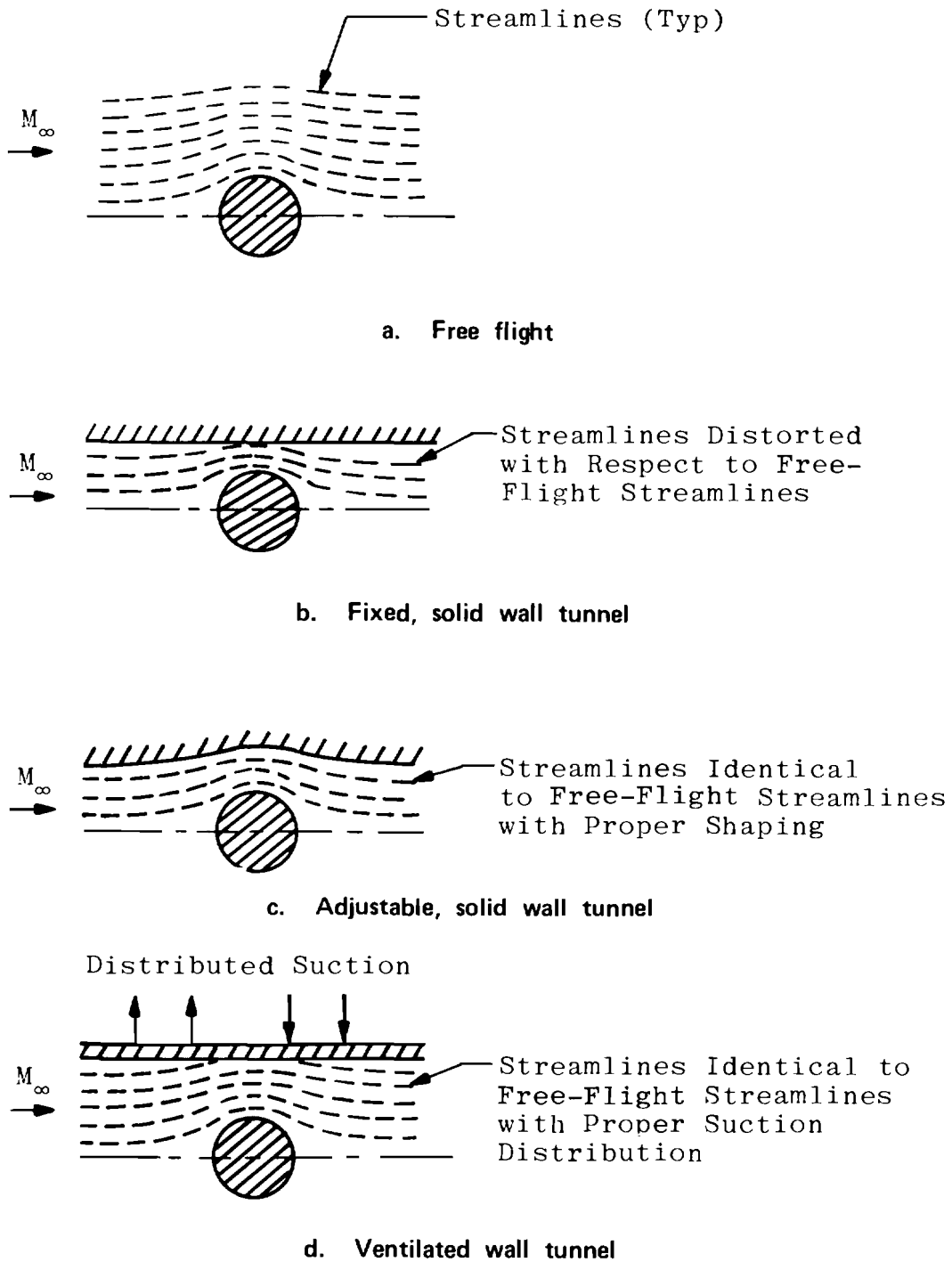
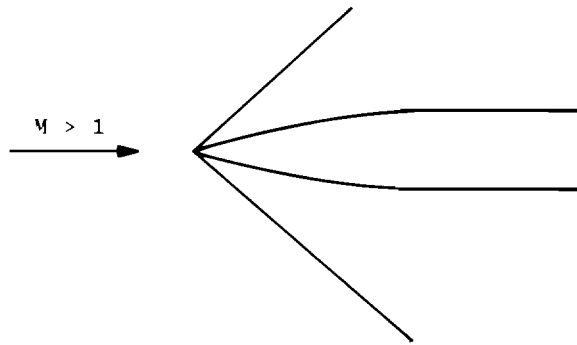
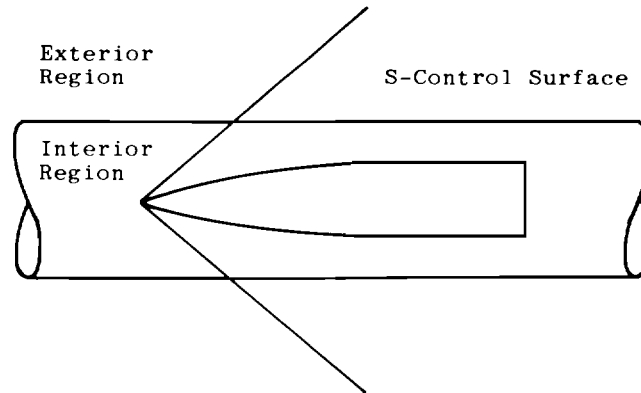


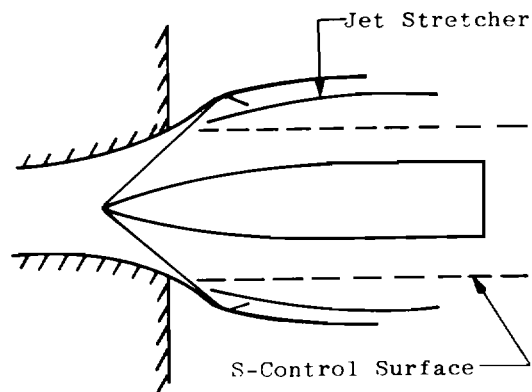
Figure 2. Schematic of near field streamline patterns for a cylinder in crossflow with various boundary conditions.



a. Unconfined supersonic flow



b. Definition of interior and exterior regions



c. Replacement of the interior region with the test cell

Figure 3. Integration of the test cell and computational domain.

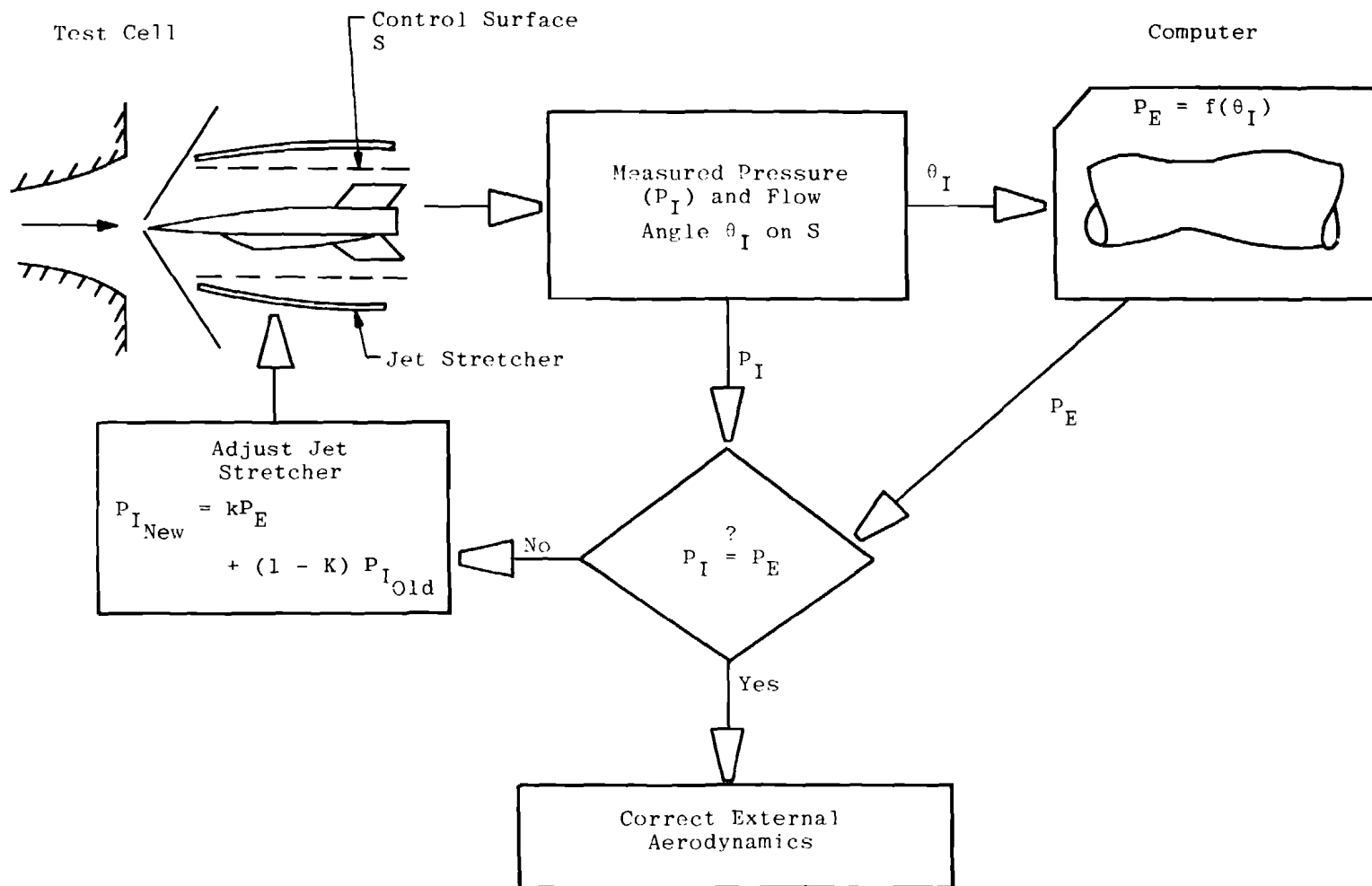


Figure 4. Iterative scheme for the adaptable jet stretcher concept.

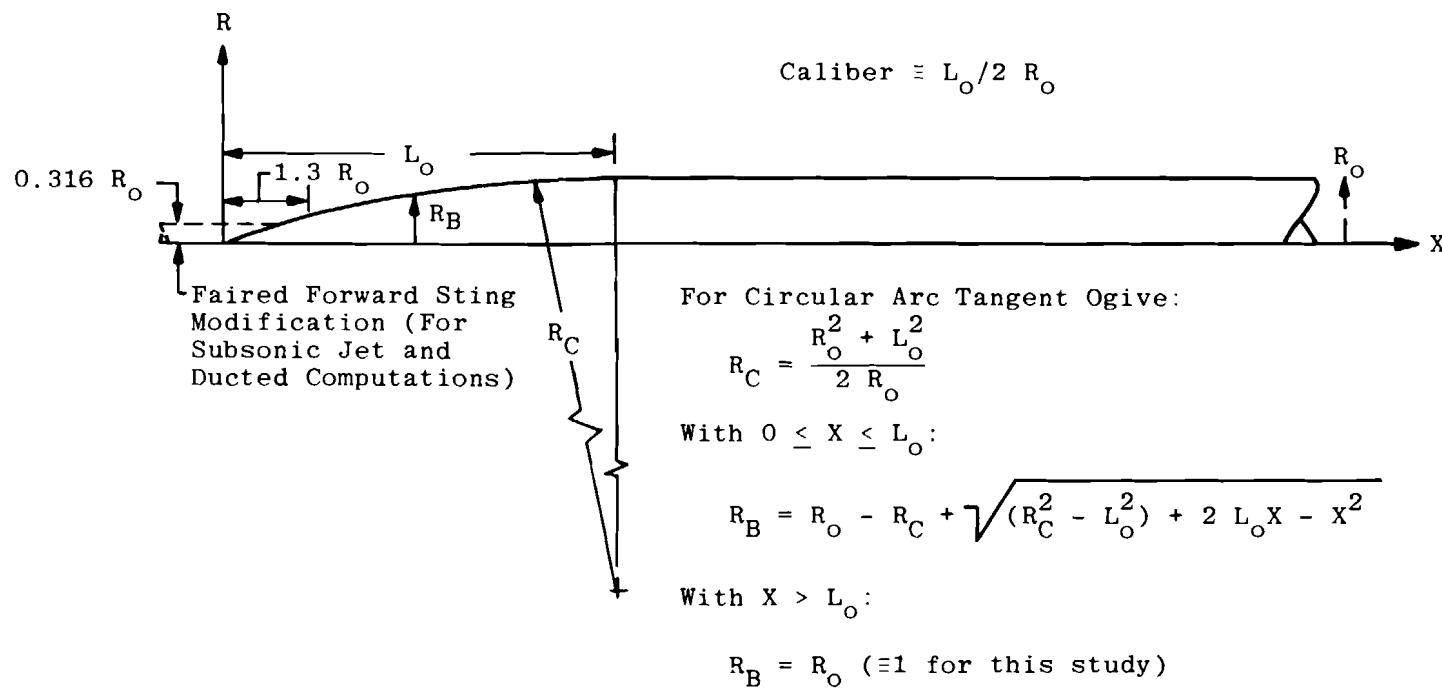


Figure 5. Details of circular arc tangent/ogive bodies used in computations.

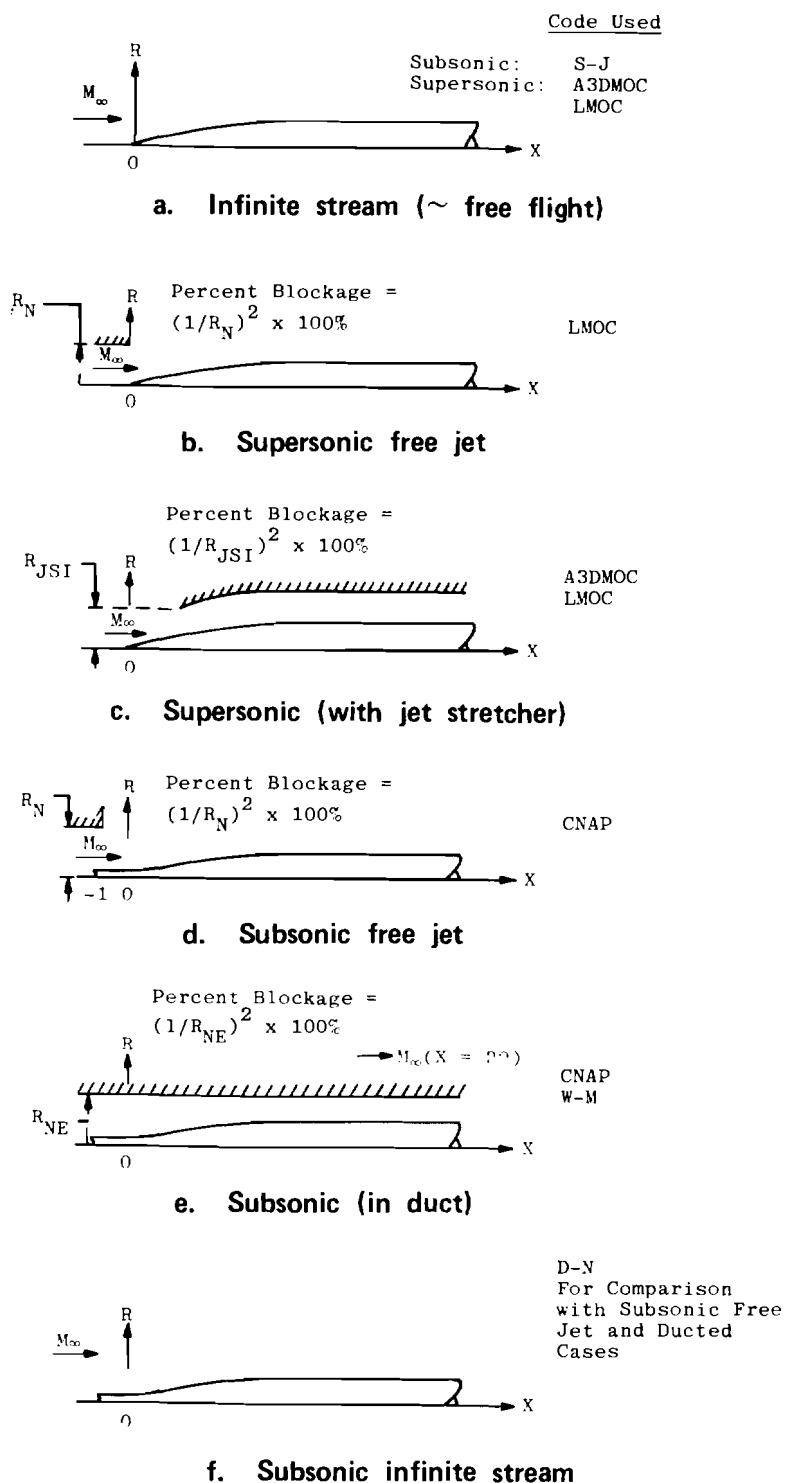
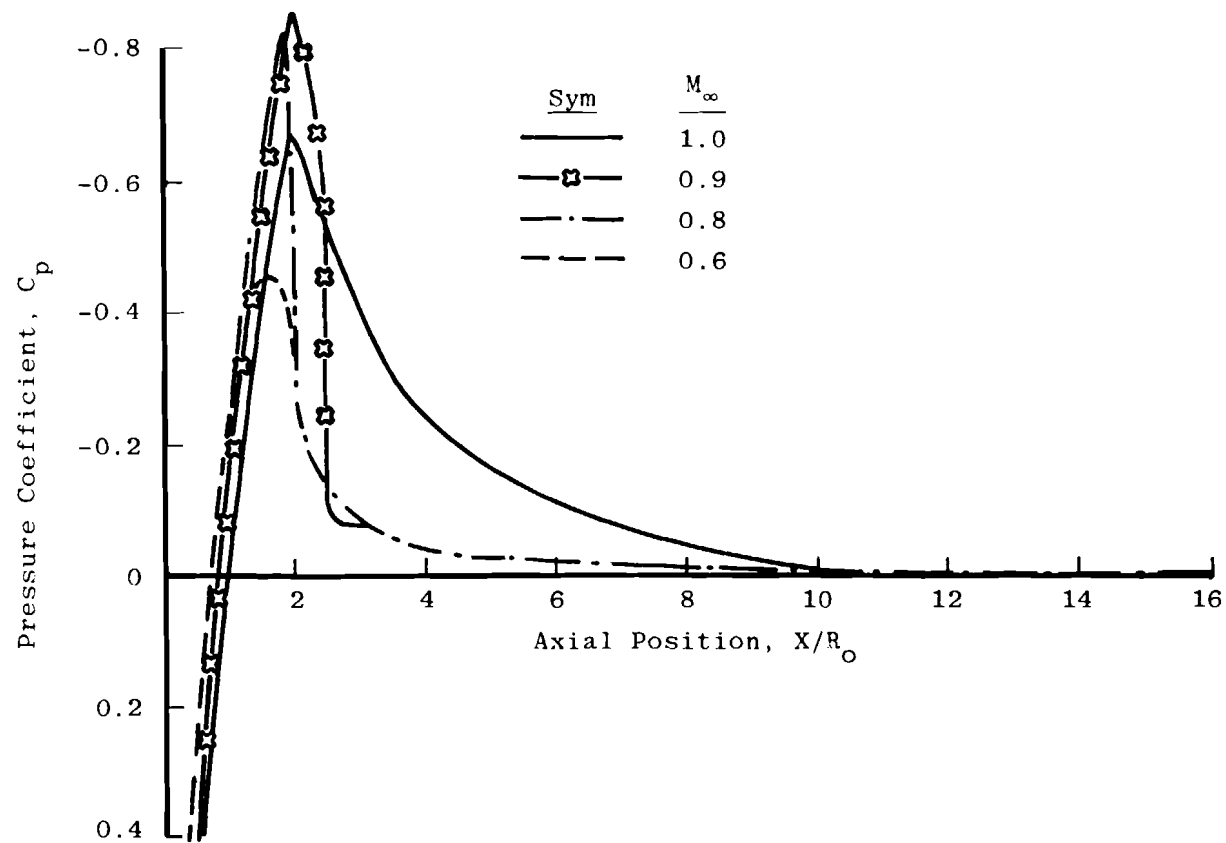
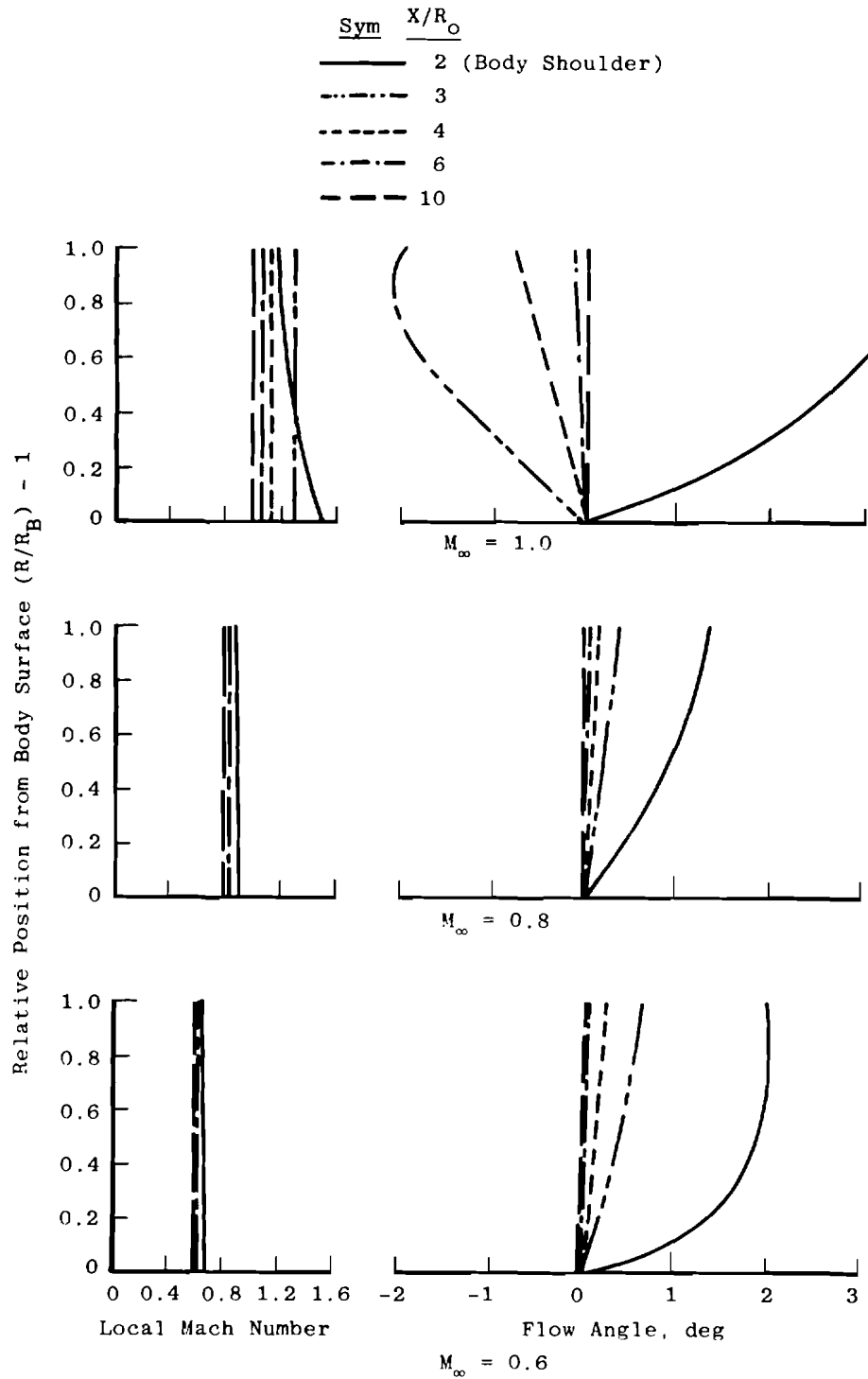


Figure 6. Boundary conditions and computer codes used in the flow-field computations.

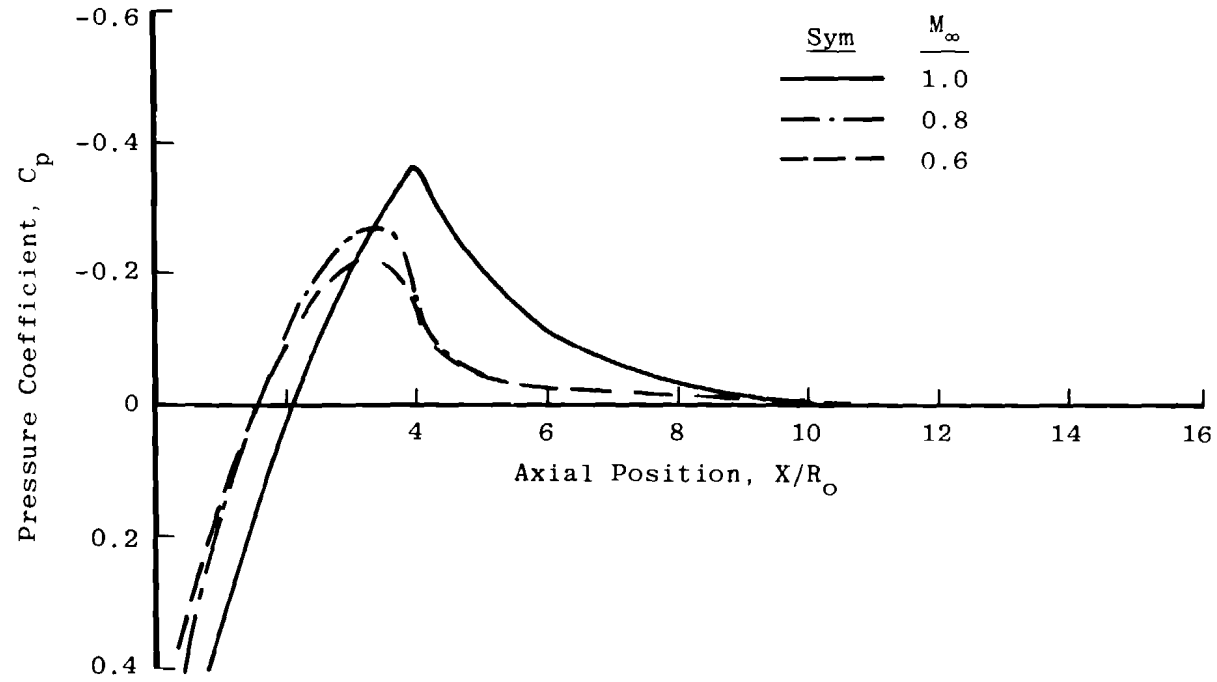


a. Body surface pressure coefficient

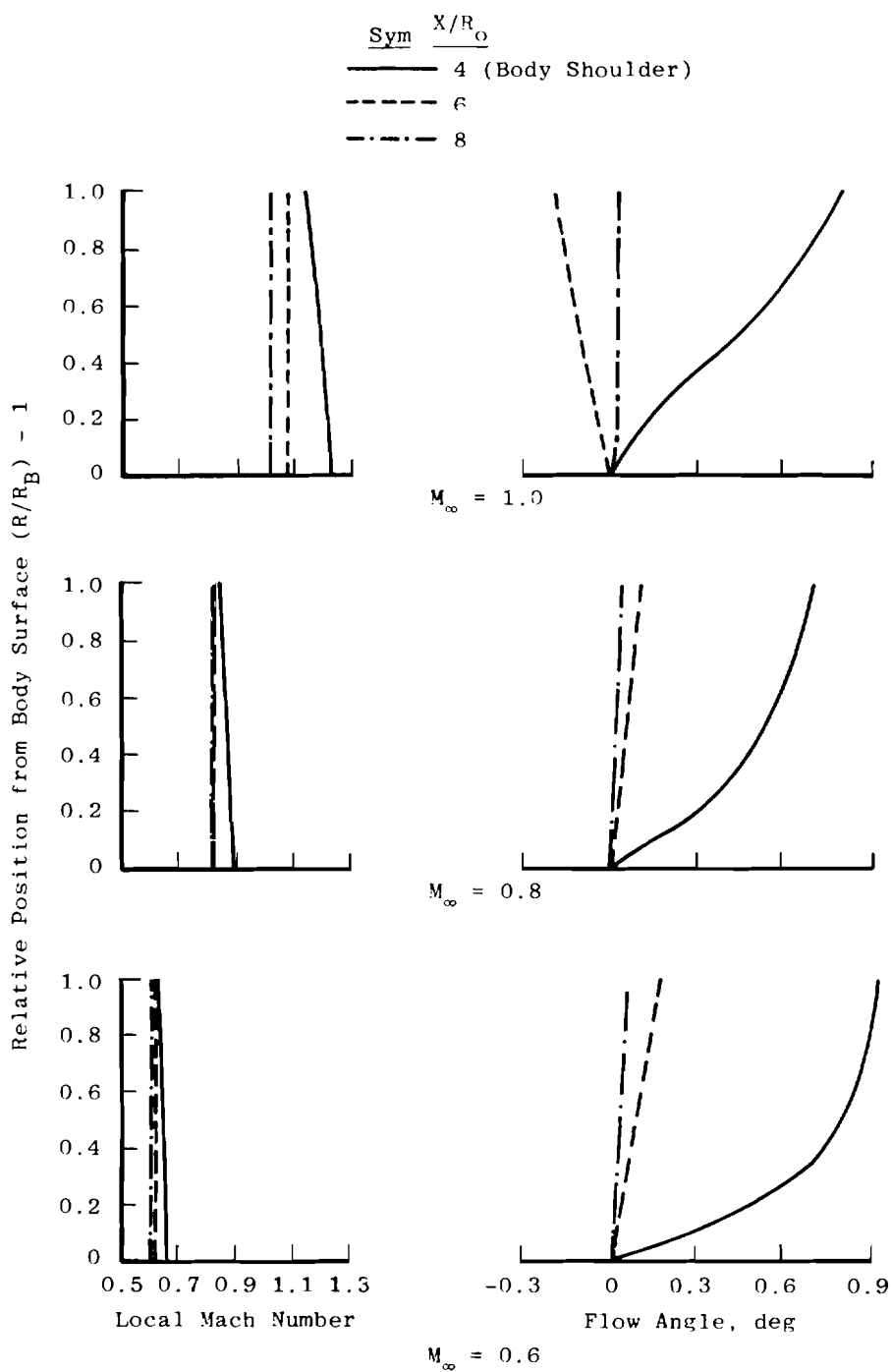
Figure 7. Flow conditions near a 1-cal tangent/ogive body with subsonic and transonic free-flight conditions.



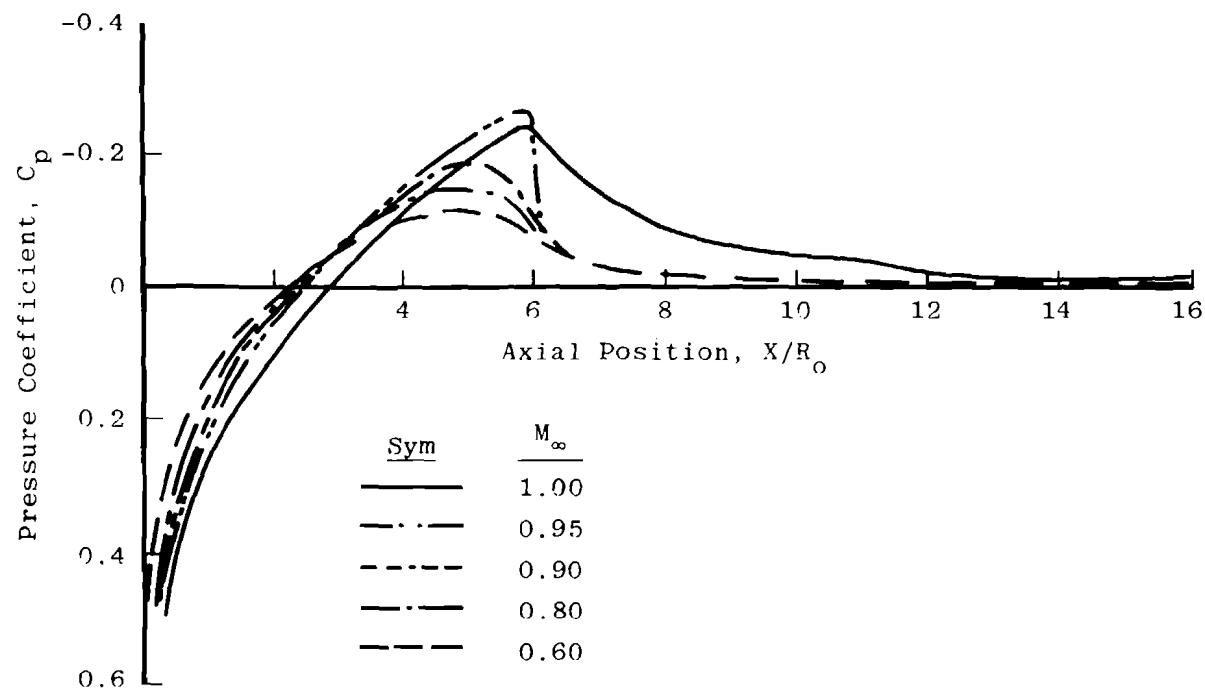
b. Local Mach number and flow angle
Figure 7. Concluded.



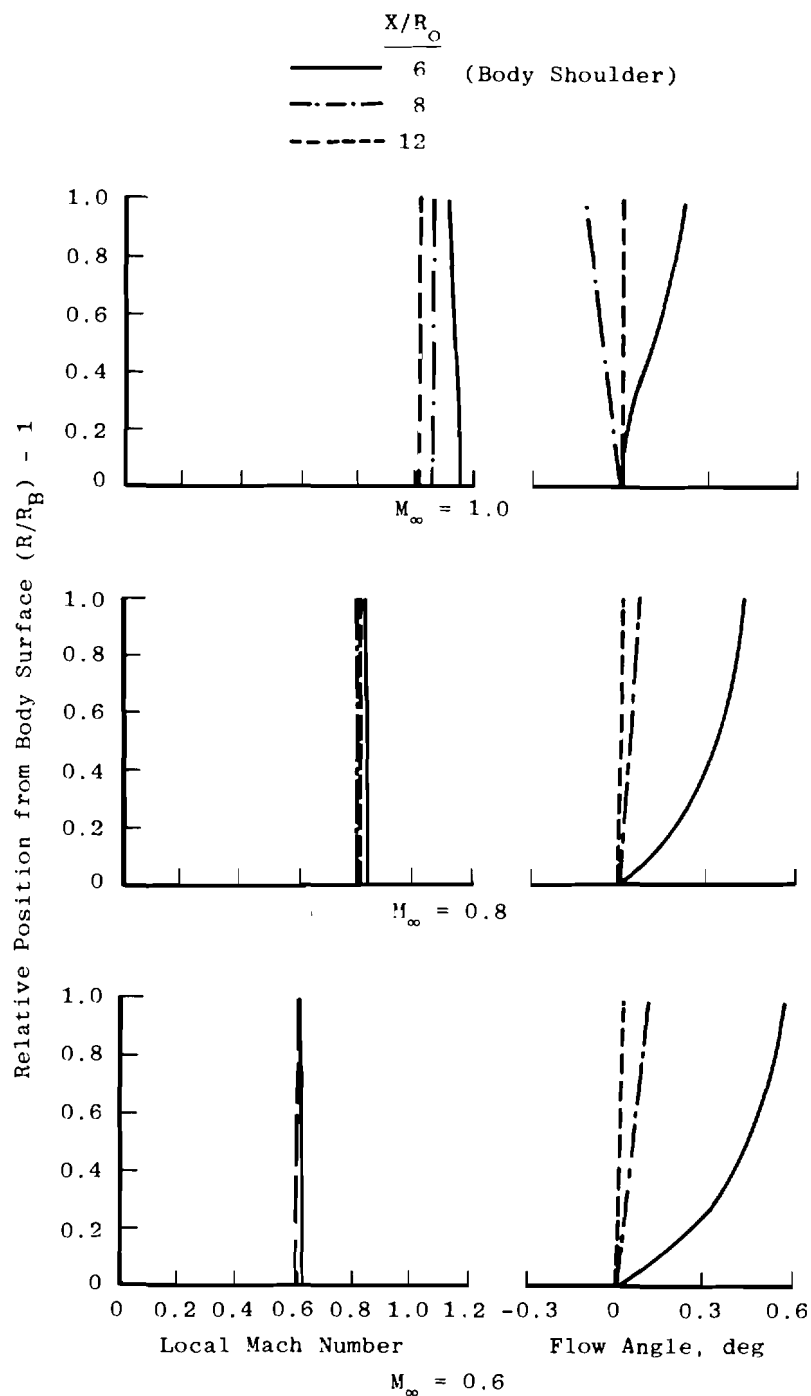
a. Body surface pressure coefficient
 Figure 8. Flow conditions near a 2-cal tangent/ogive body with subsonic and transonic free-flight conditions.



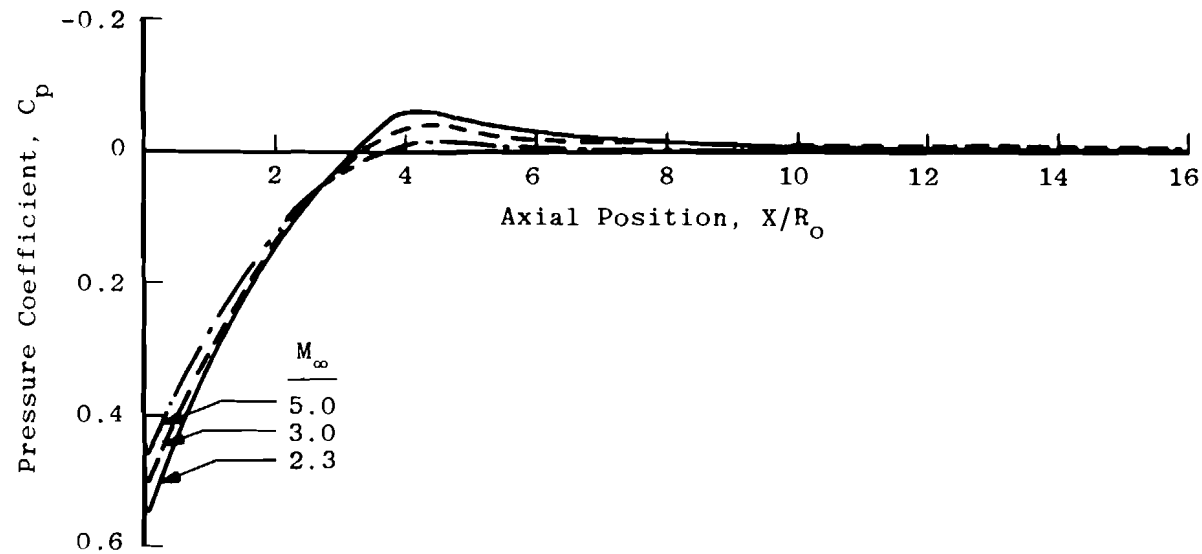
b. Local Mach number and flow angle
Figure 8. Concluded.



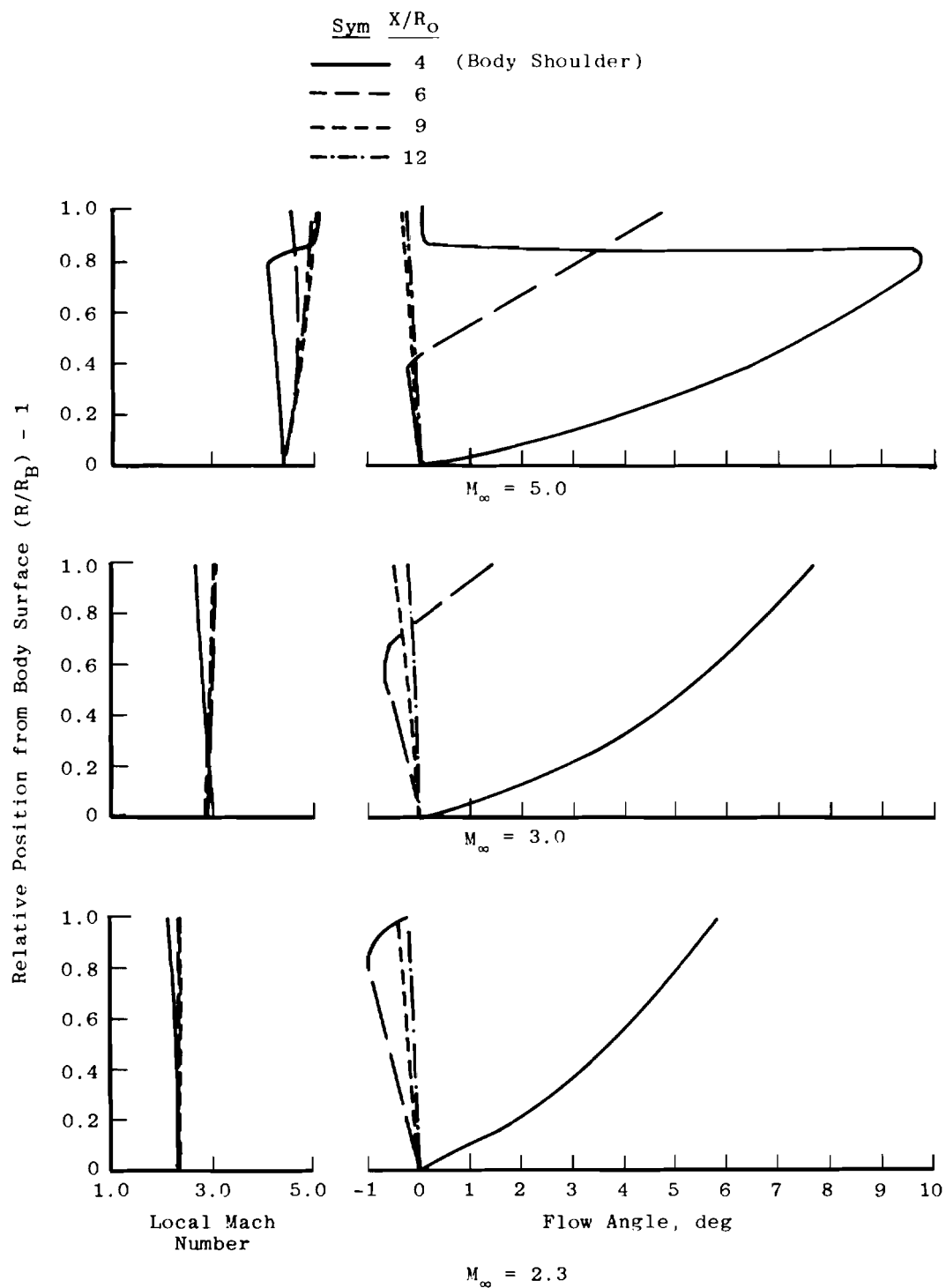
a. Body surface pressure coefficient
 Figure 9. Flow conditions near a 3-cal tangent/ogive body with subsonic and transonic free-flight conditions.



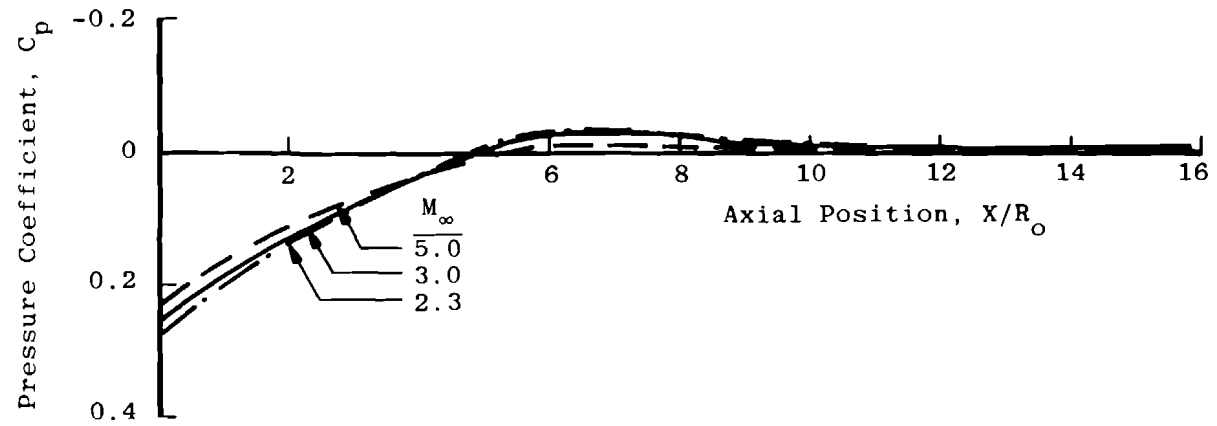
b. Local Mach number and flow angle
 Figure 9. Concluded.



a. Body surface pressure coefficient
 Figure 10. Flow conditions near a 2-cal tangent/ogive body
 with supersonic free-flight conditions.

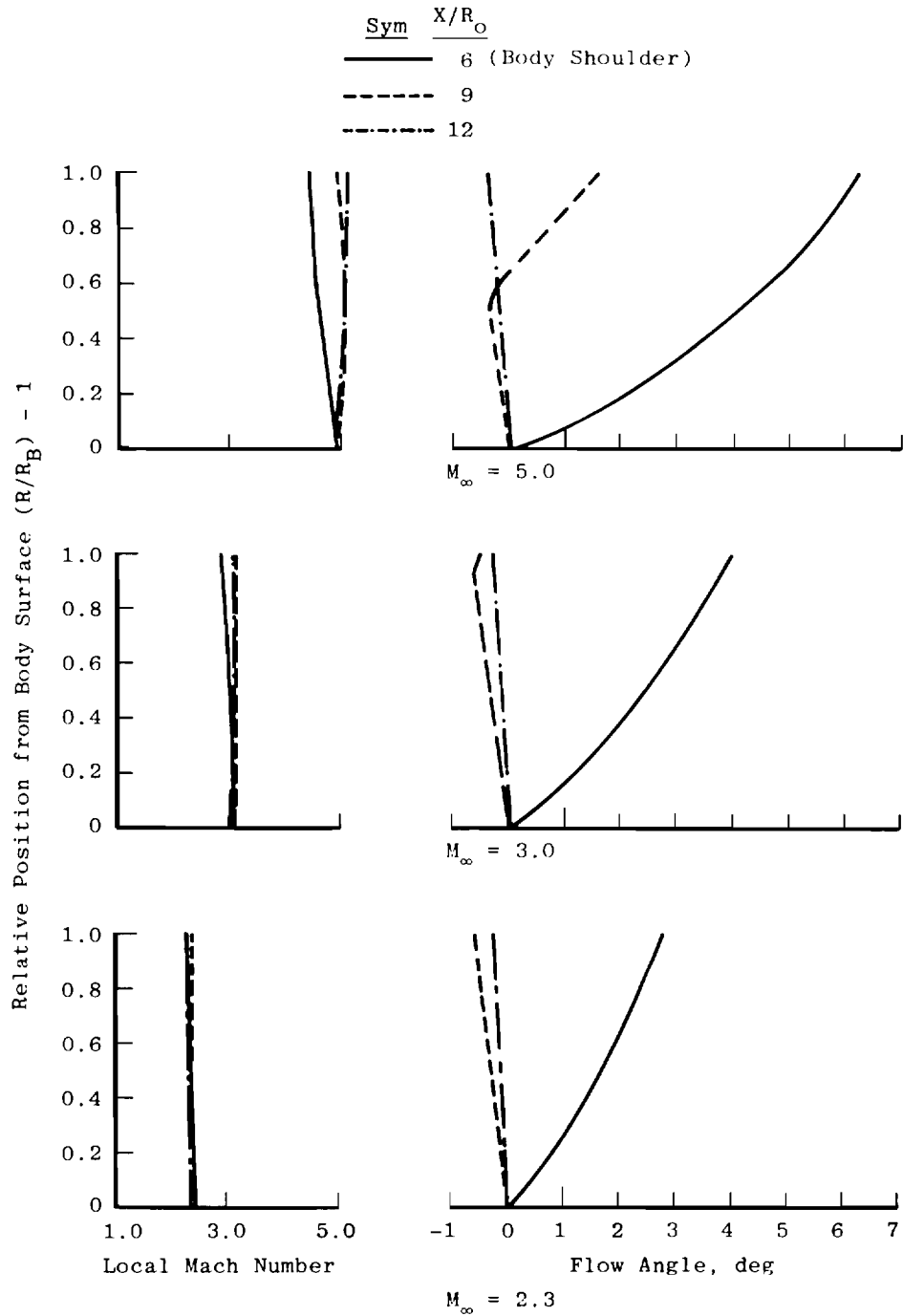


b. Local Mach number and flow angle
Figure 10. Concluded.



a. Body surface pressure coefficient

Figure 11. Flow conditions near a 3-cal tangent/ogive body with supersonic free-flight conditions.



b. Local Mach number and flow angle
Figure 11. Concluded.

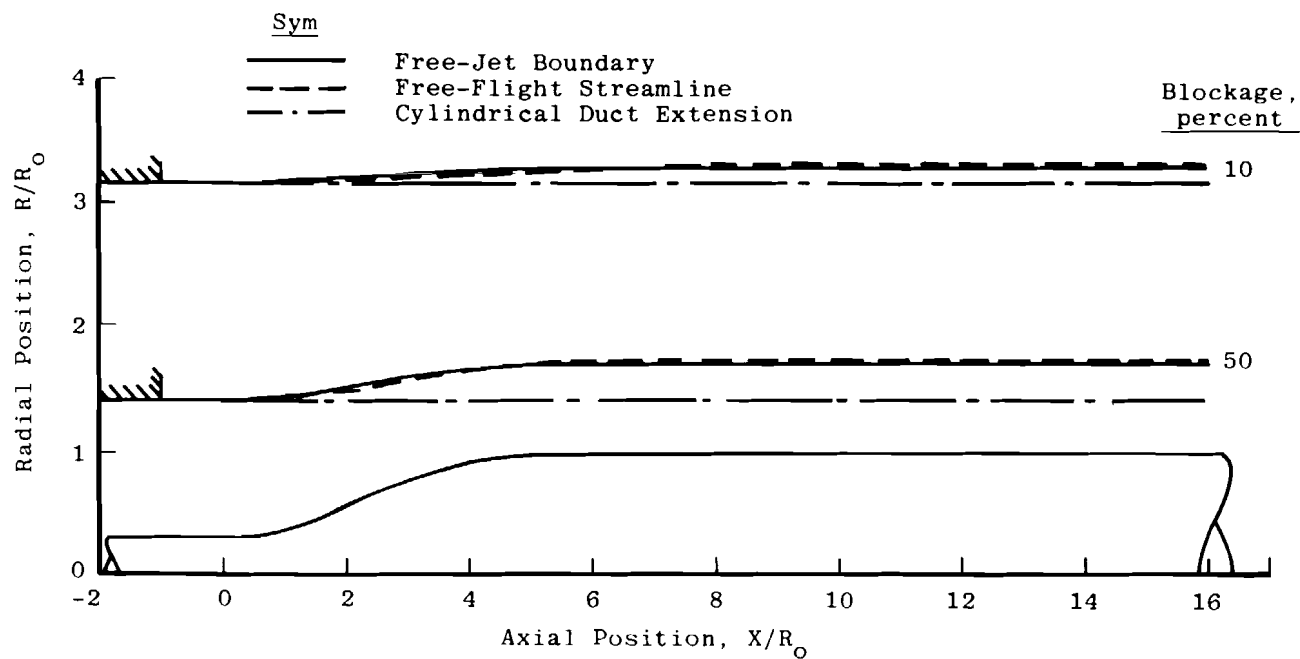
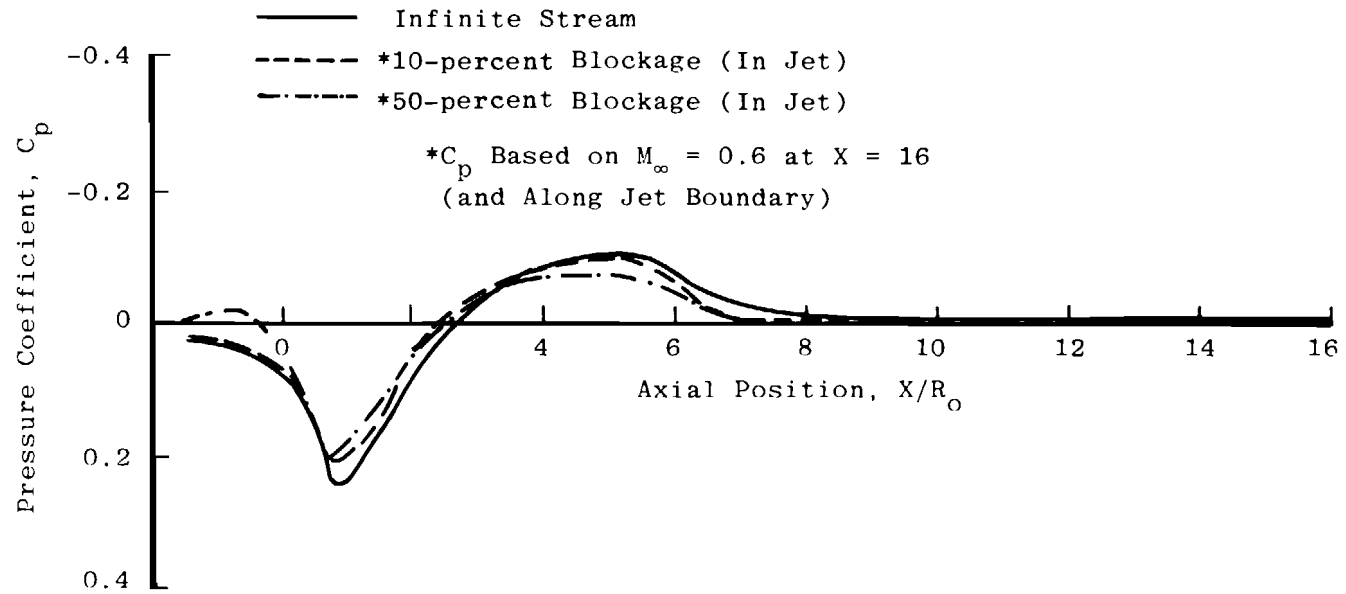
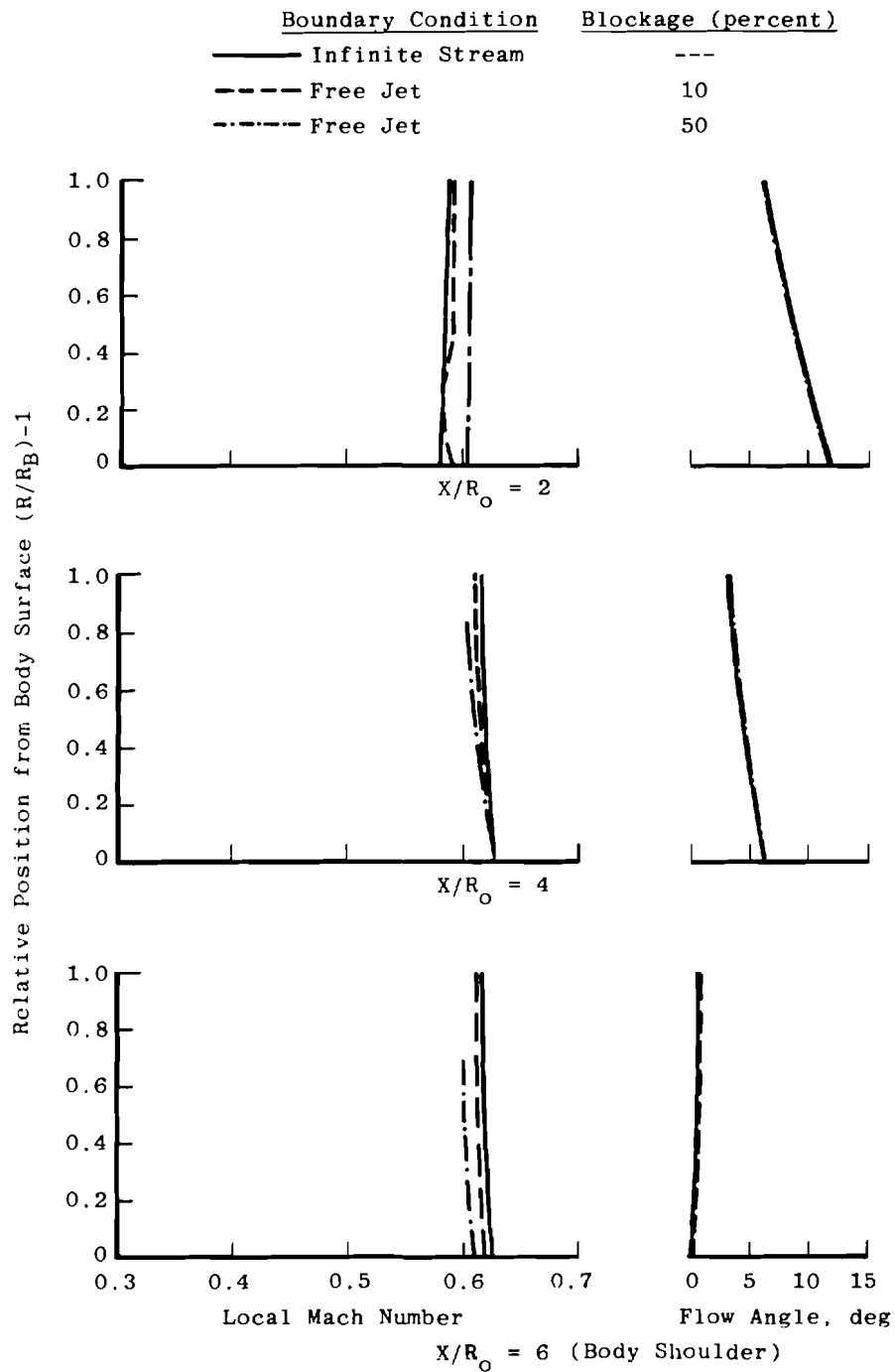


Figure 12. Comparison of free-jet boundaries, free-flight streamlines, and cylindrical duct extensions considered in the subsonic computations (3-cal tangent/ogive, $M_\infty = 0.6$).

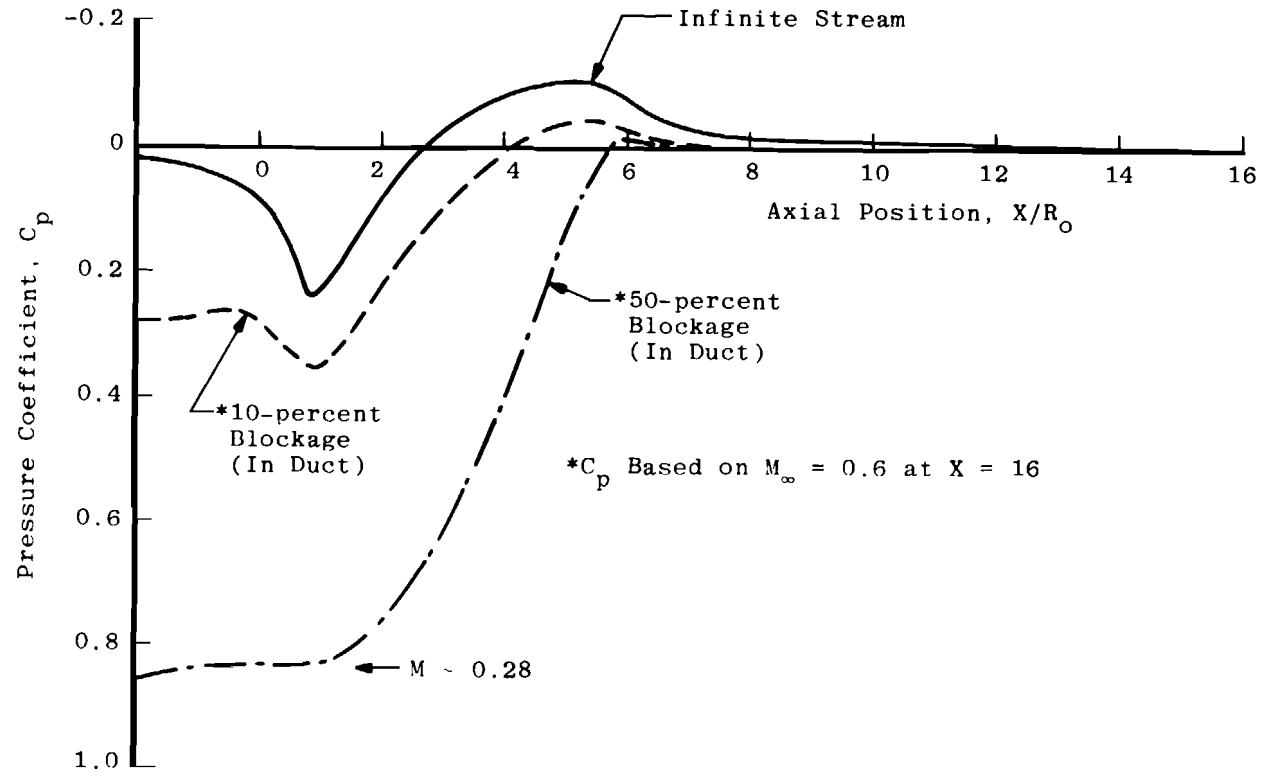


a. Body surface pressure coefficients
 Figure 13. Flow conditions near a 3-cal tangent/ogive body
 with $M_\infty = 0.6$ free-flight and free-jet operation.

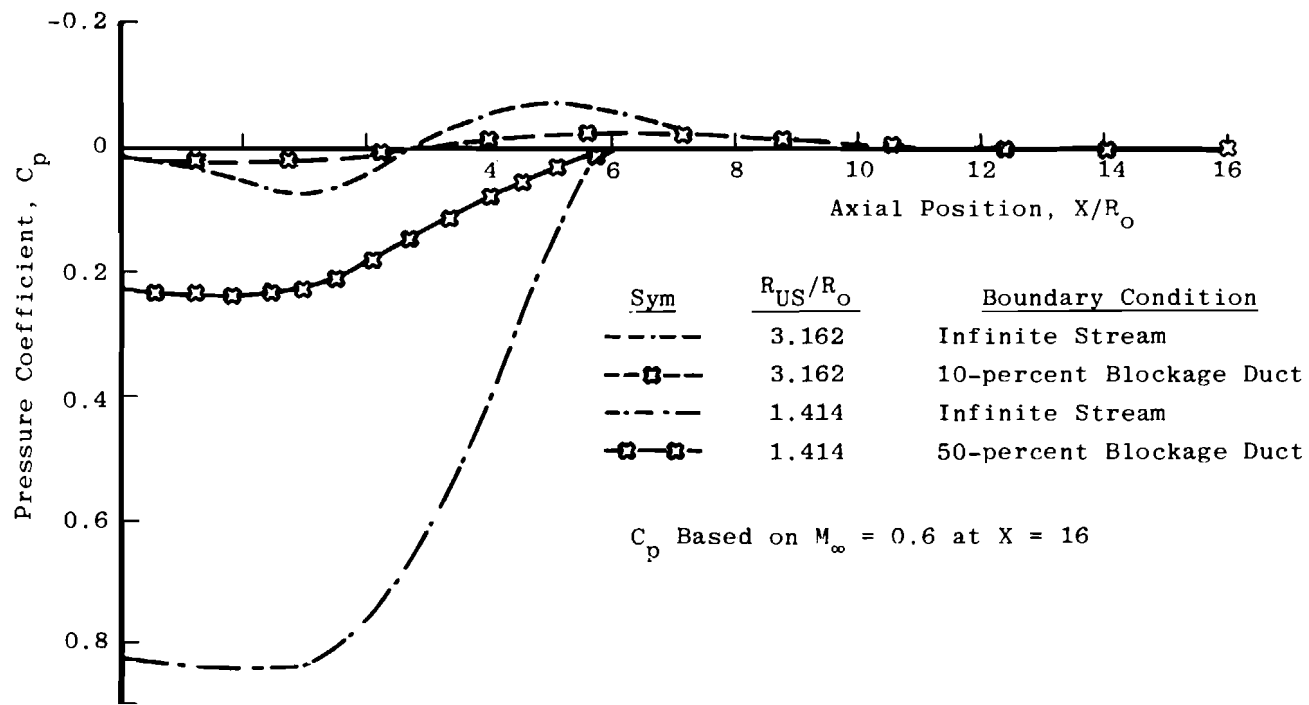


b. Forebody Mach number and flow angle variations in free-flight and free-jet environments.

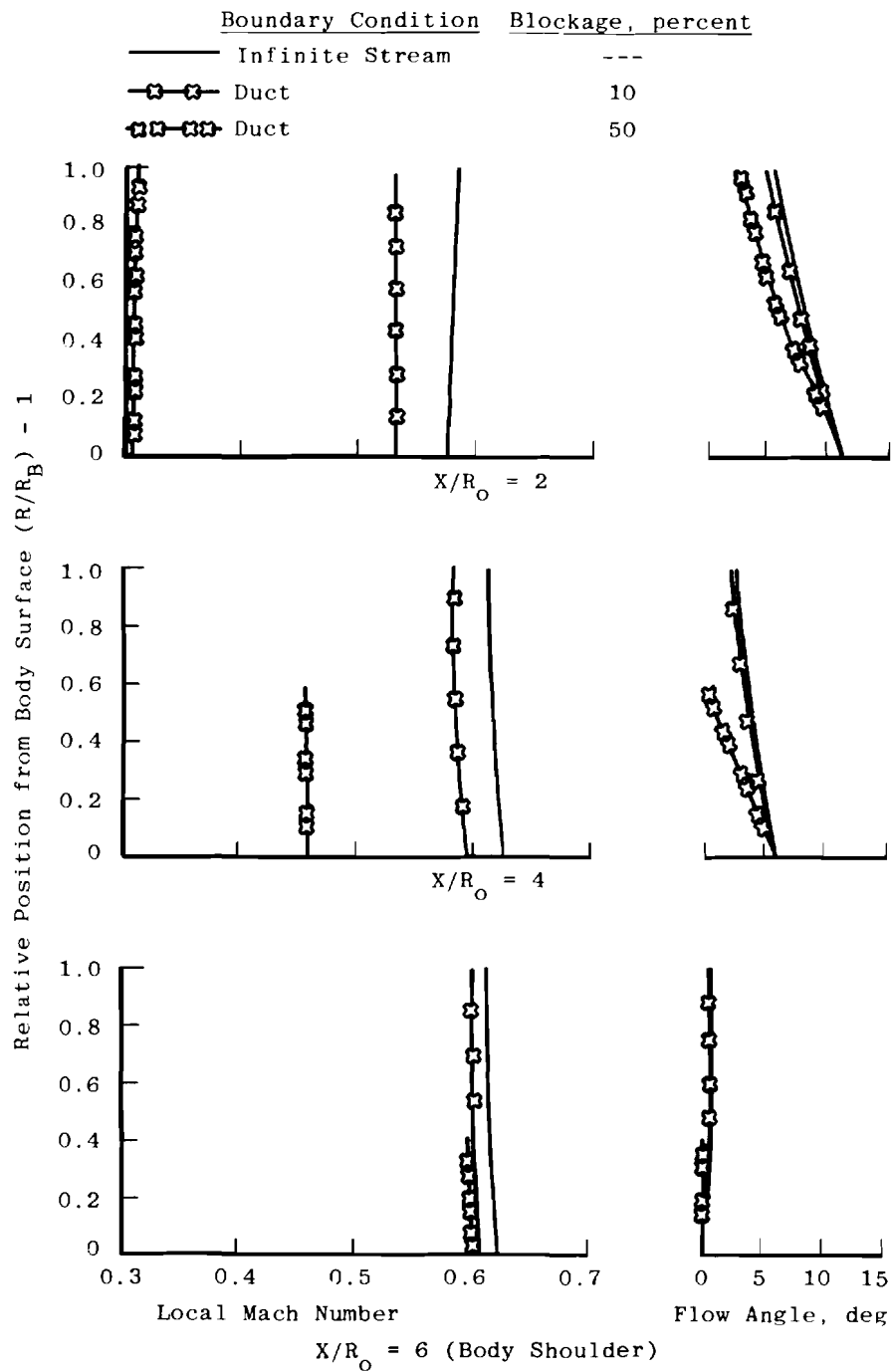
Figure 13. Concluded.



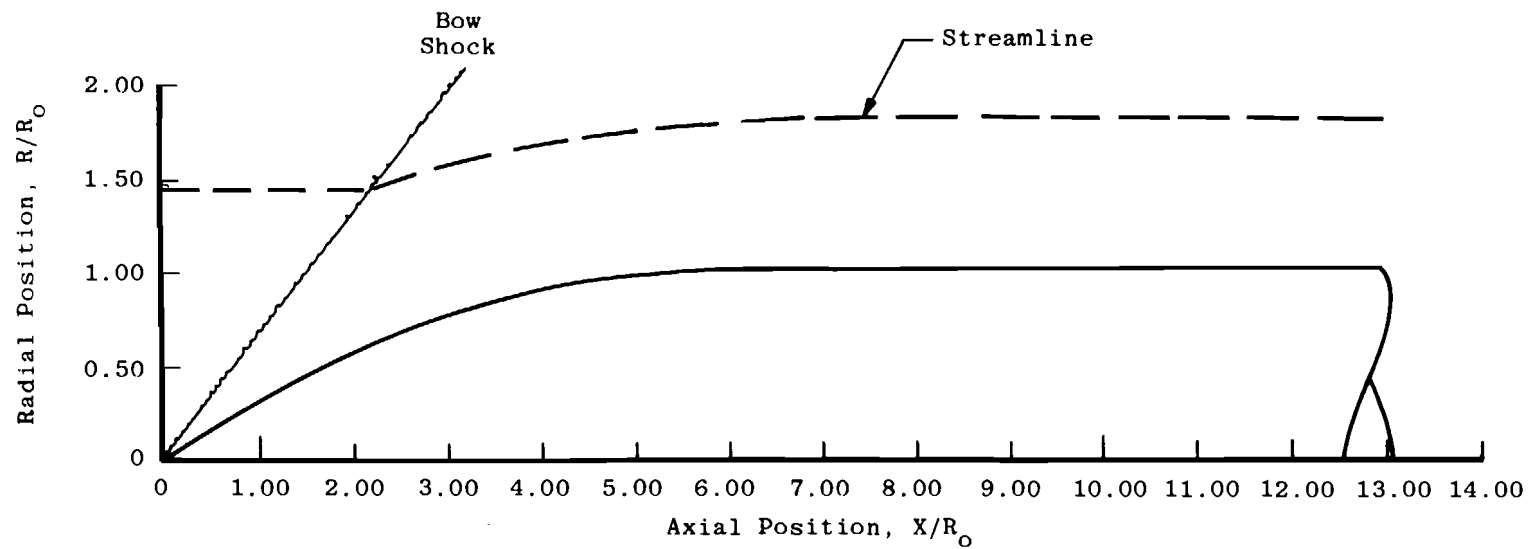
a. Body surface pressure coefficients
 Figure 14. Flow conditions near a 3-cal tangent/ogive body with $M_\infty = 0.6$ free-flight and ducted operation.



b. Comparison of pressure coefficients on the duct wall and along a comparable surface in free flight.
Figure 14. Continued.

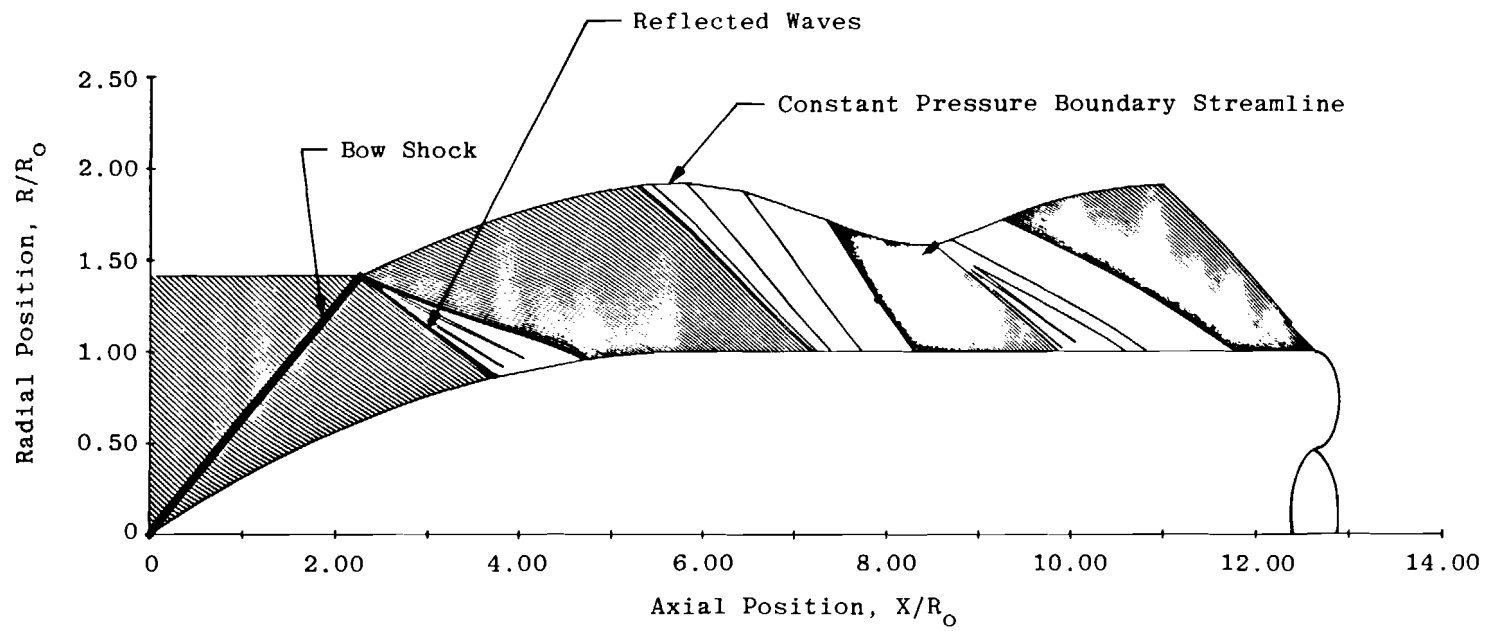


c. Forebody Mach number and flow angle variations
Figure 14. Concluded.

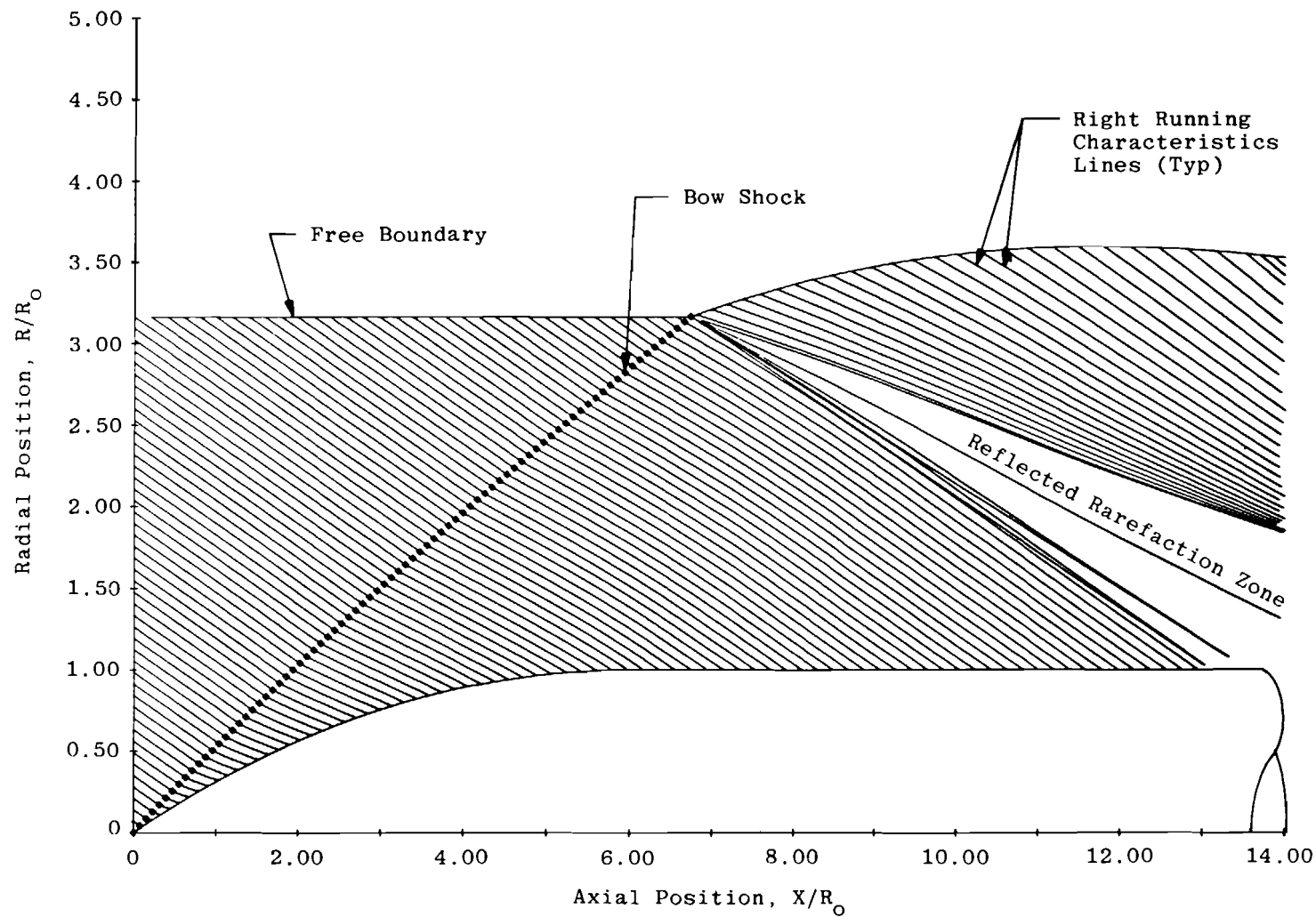


a. Free flight

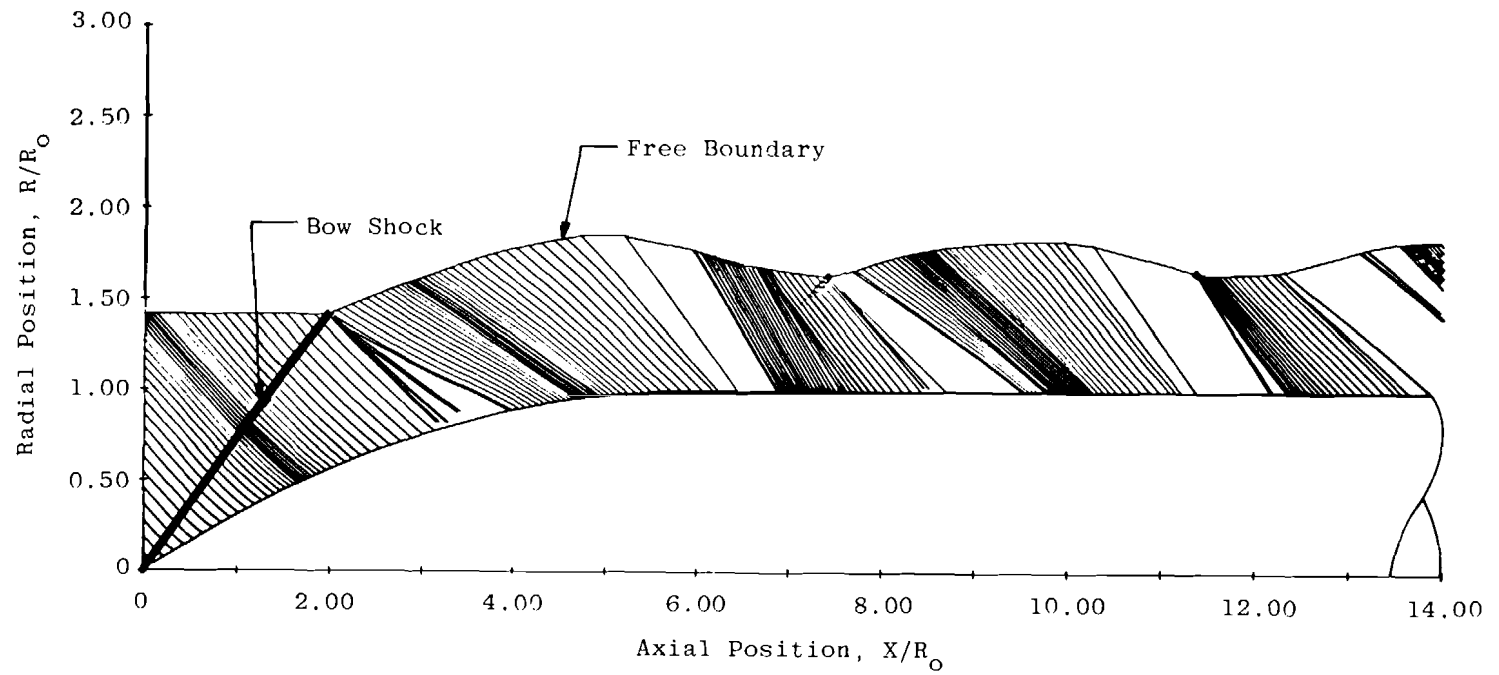
Figure 15. Comparison of free-jet and free-flight flow details
(50-percent blockage 3-cal tangent/ogive.)



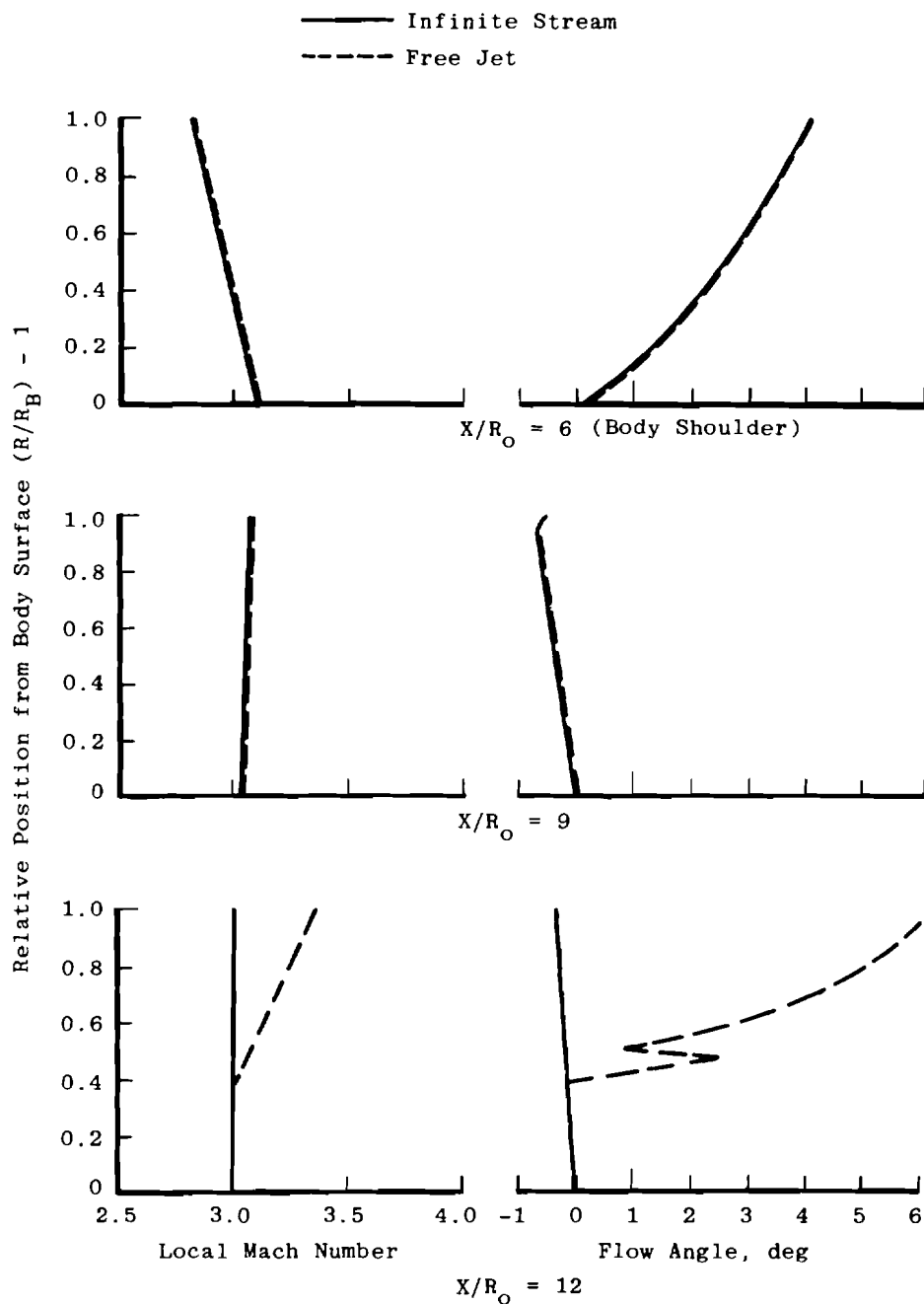
b. Free jet
Figure 15. Concluded.



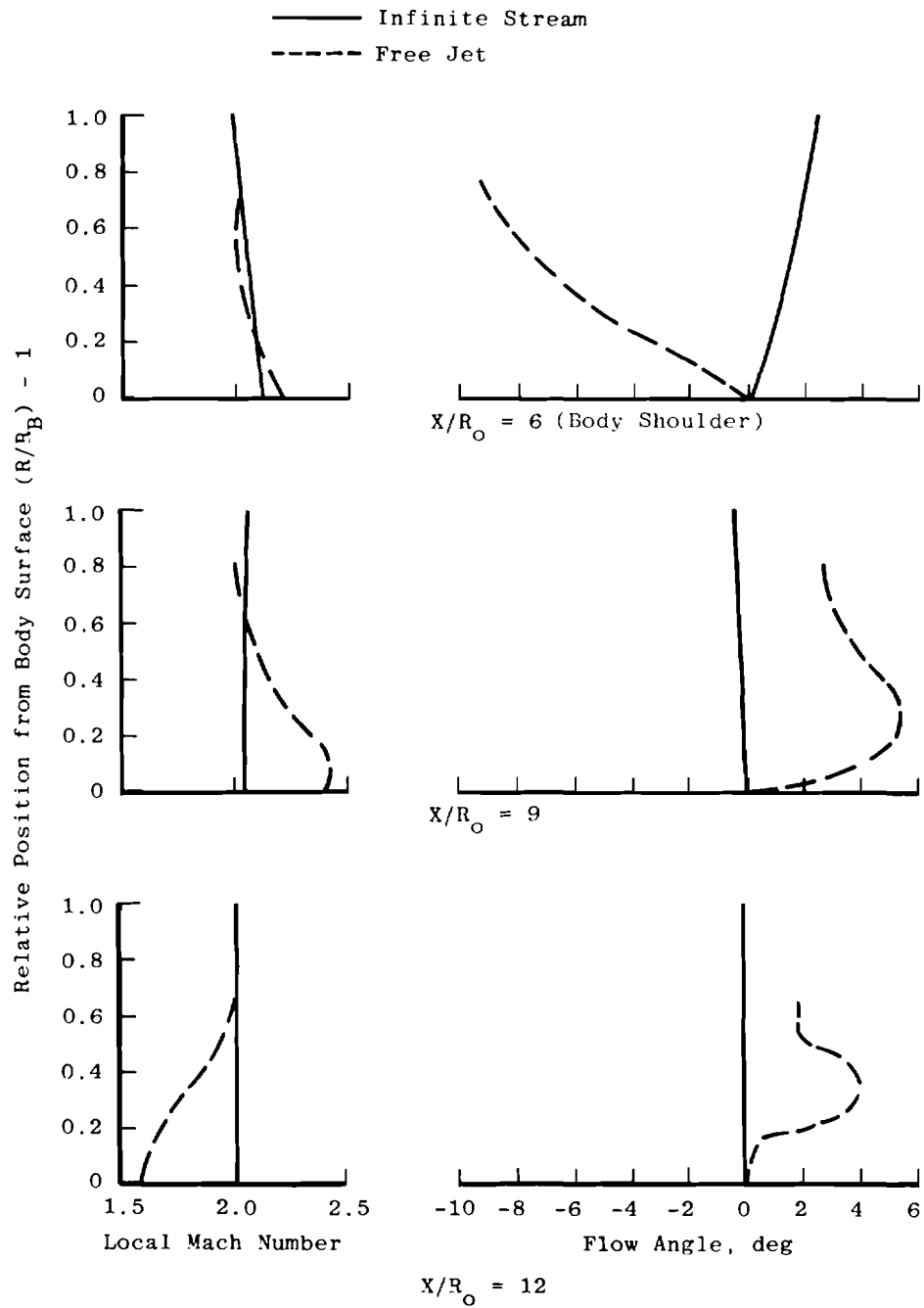
a. 10-percent blockage body with $M_\infty = 3.0$
 Figure 16. Flow-field details produced by a 3-cal tangent/ogive body in a supersonic free jet.



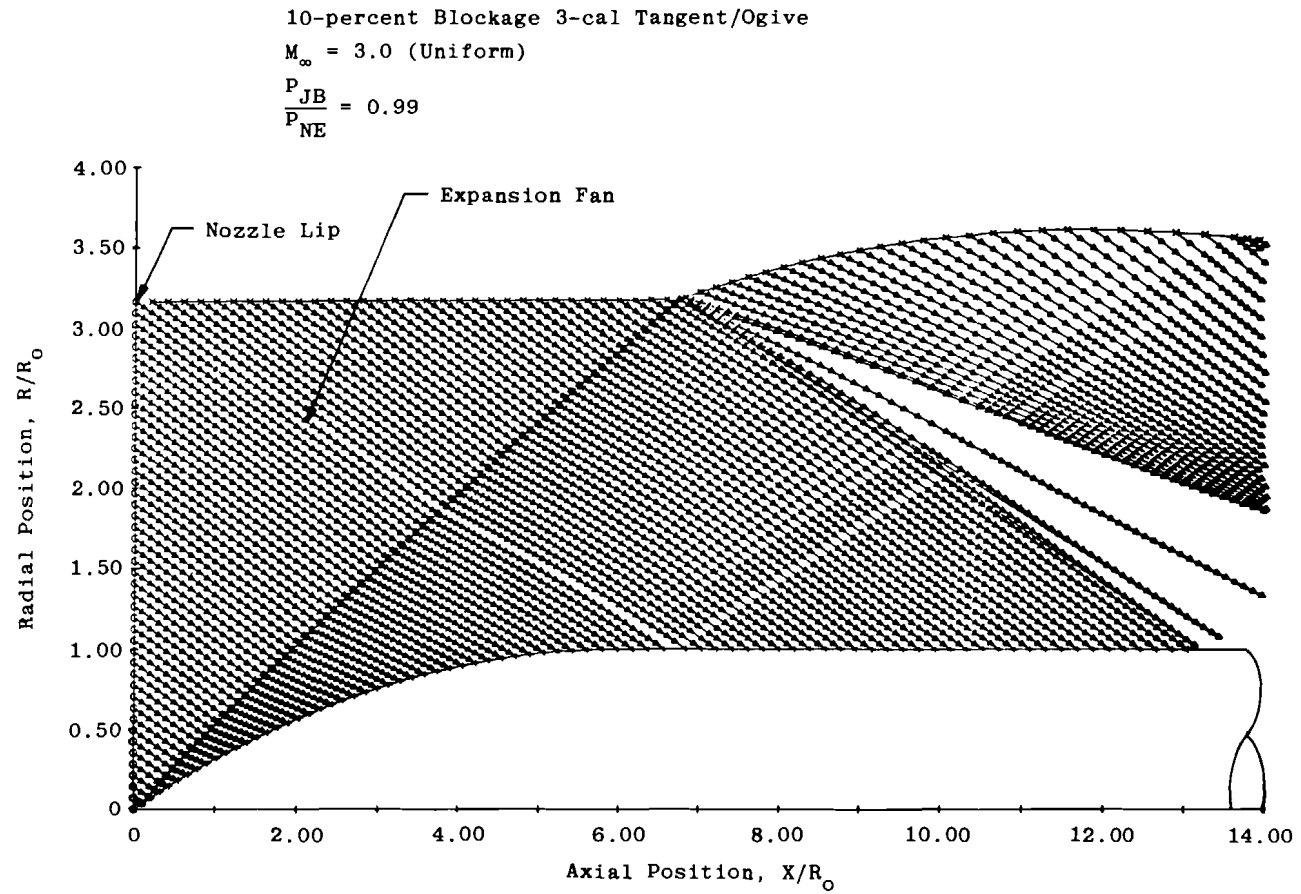
b. 50-percent blockage body with $M_\infty = 2.0$
Figure 16. Concluded.



a. 10-percent blockage, $M_\infty = 3.0$
 Figure 17. Comparison of flow-field conditions near a 3-cal tangent/ogive body with supersonic free-jet and free-flight conditions.

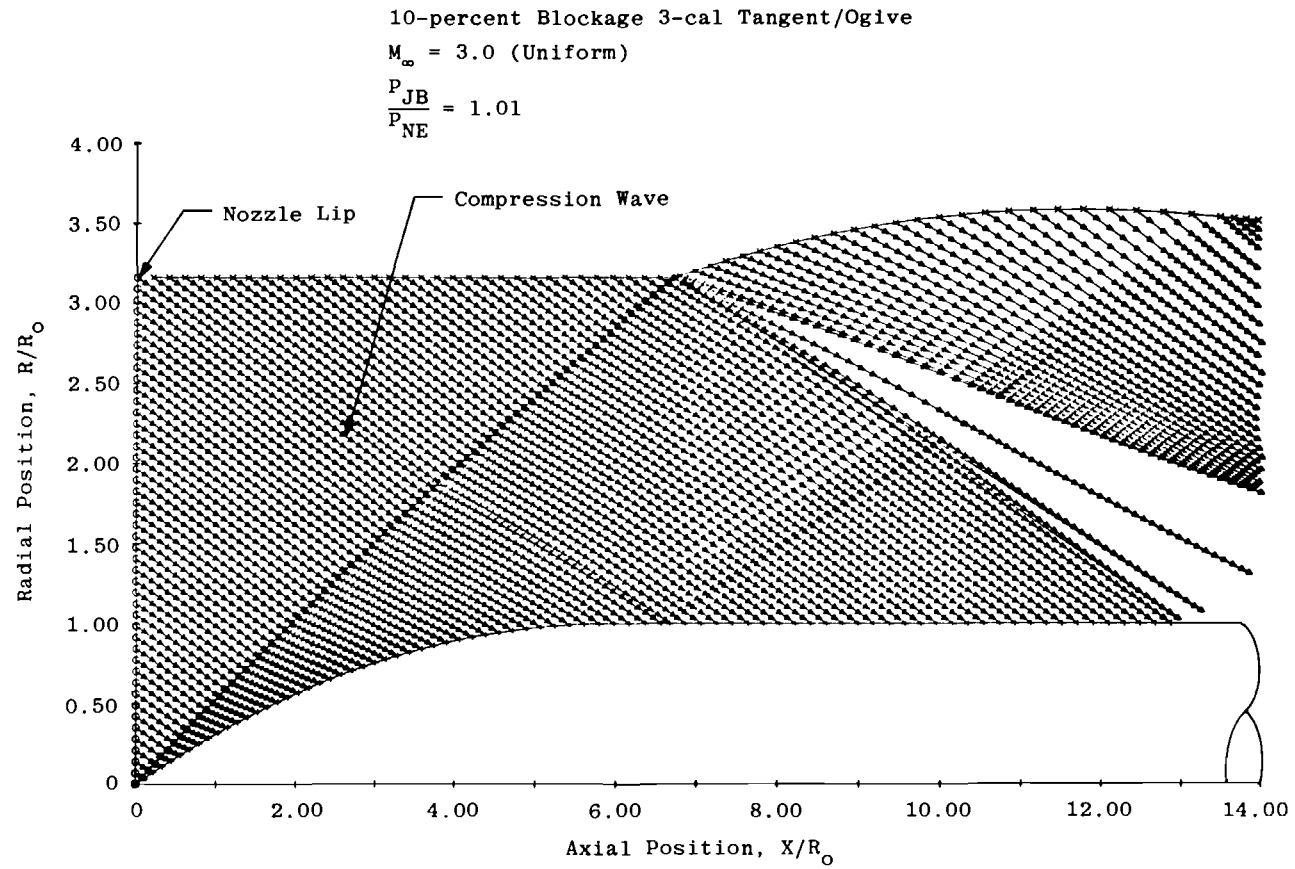


b. 50-percent blockage, $M_\infty = 2.0$
 Figure 17. Concluded.

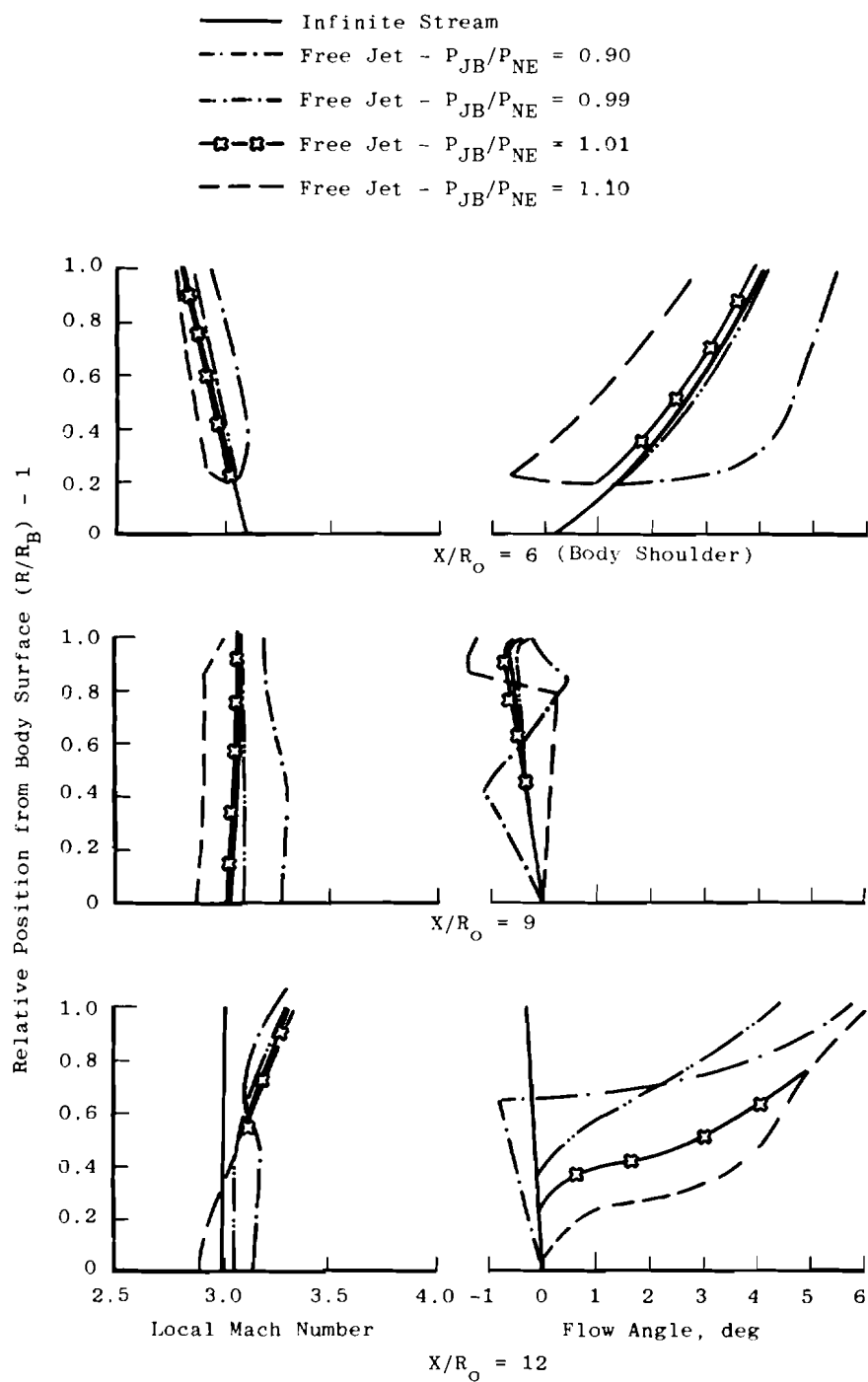


a. Underexpanded nozzle flow

Figure 18. Extraneous waves introduced by pressure mismatch at free-jet nozzle exit.



b. Overexpanded nozzle flow
 Figure 18. Continued.



c. Flow-field conditions
 Figure 18. Concluded.

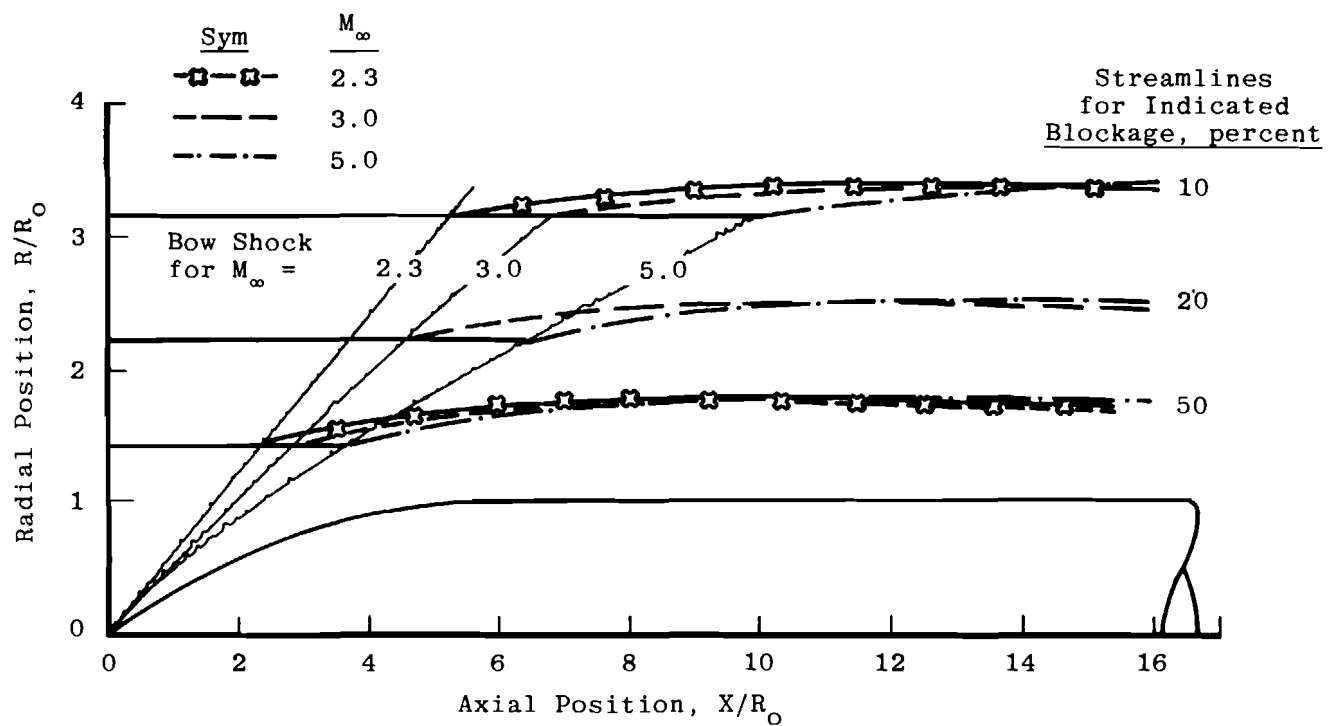
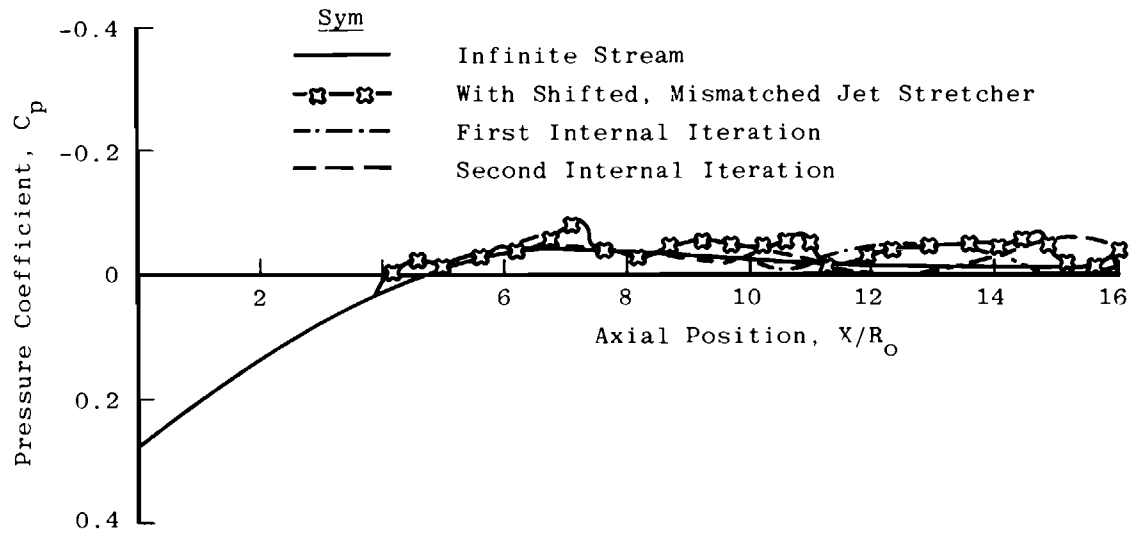
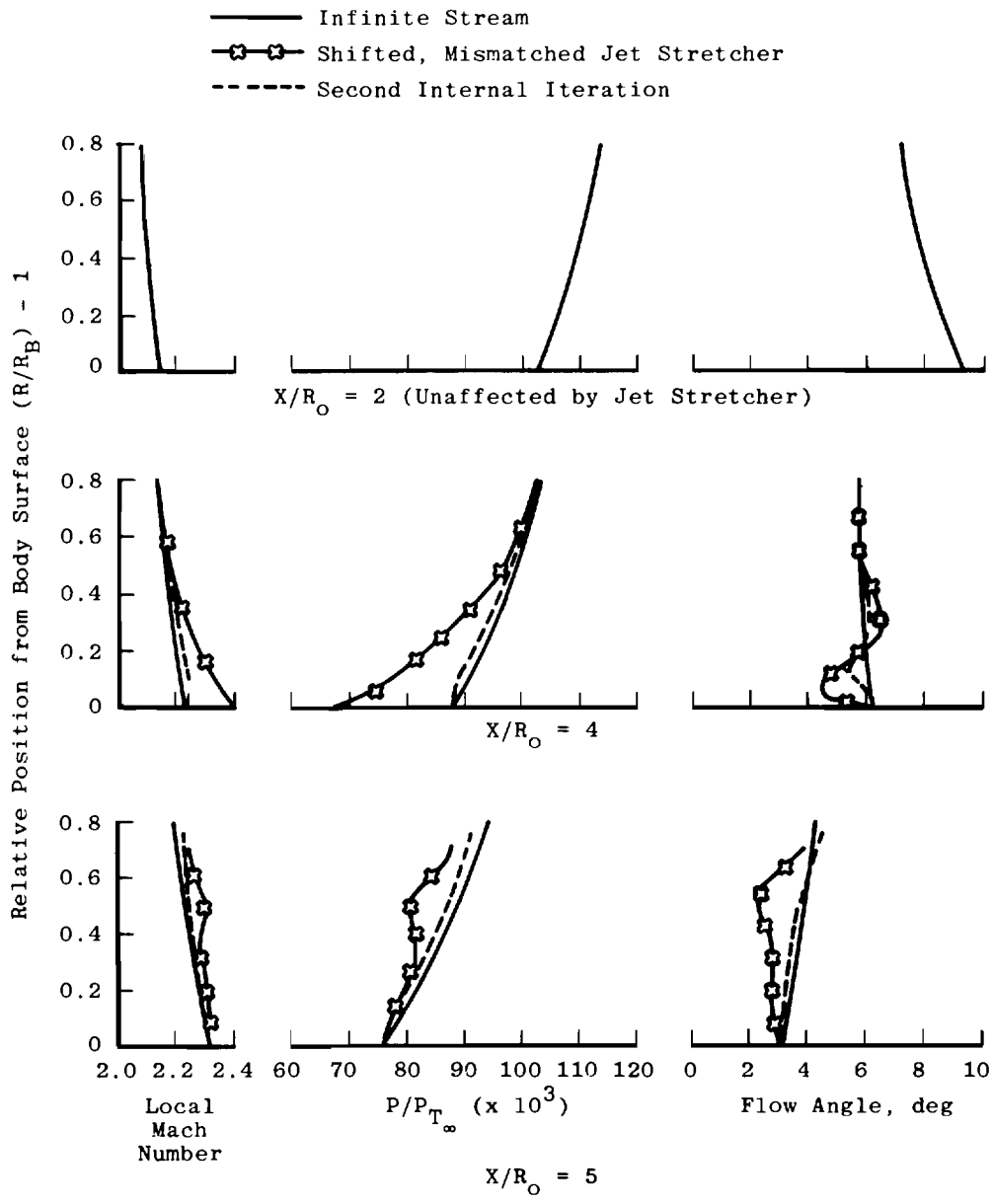


Figure 19. Streamline trajectories at various supersonic free-flight conditions about a 3-cal tangent/ogive body.

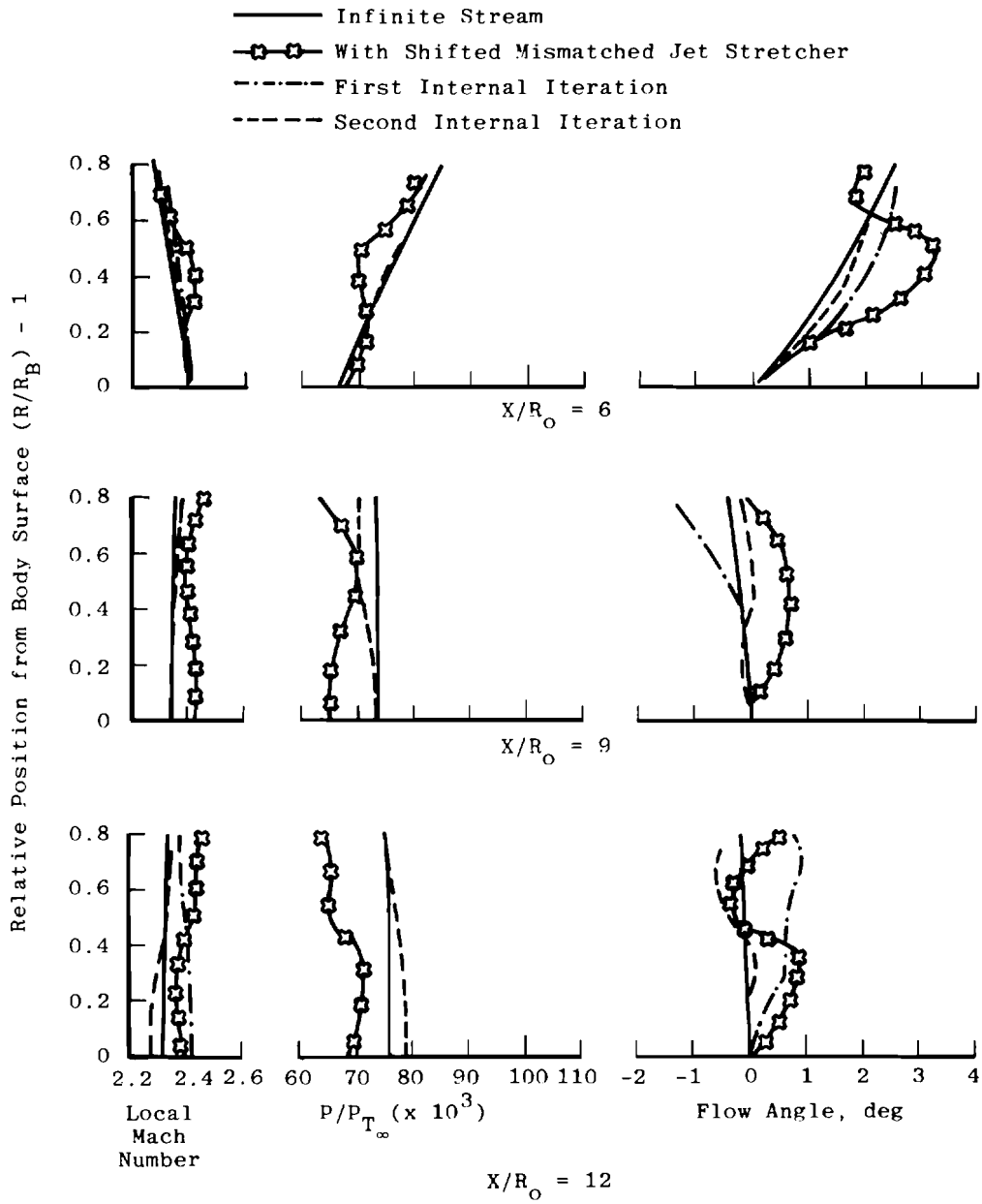


a. Comparison of body pressure coefficients
 Figure 20. Computed flow conditions near a 3-cal tangent/ogive body with iterative jet stretcher adjustments.

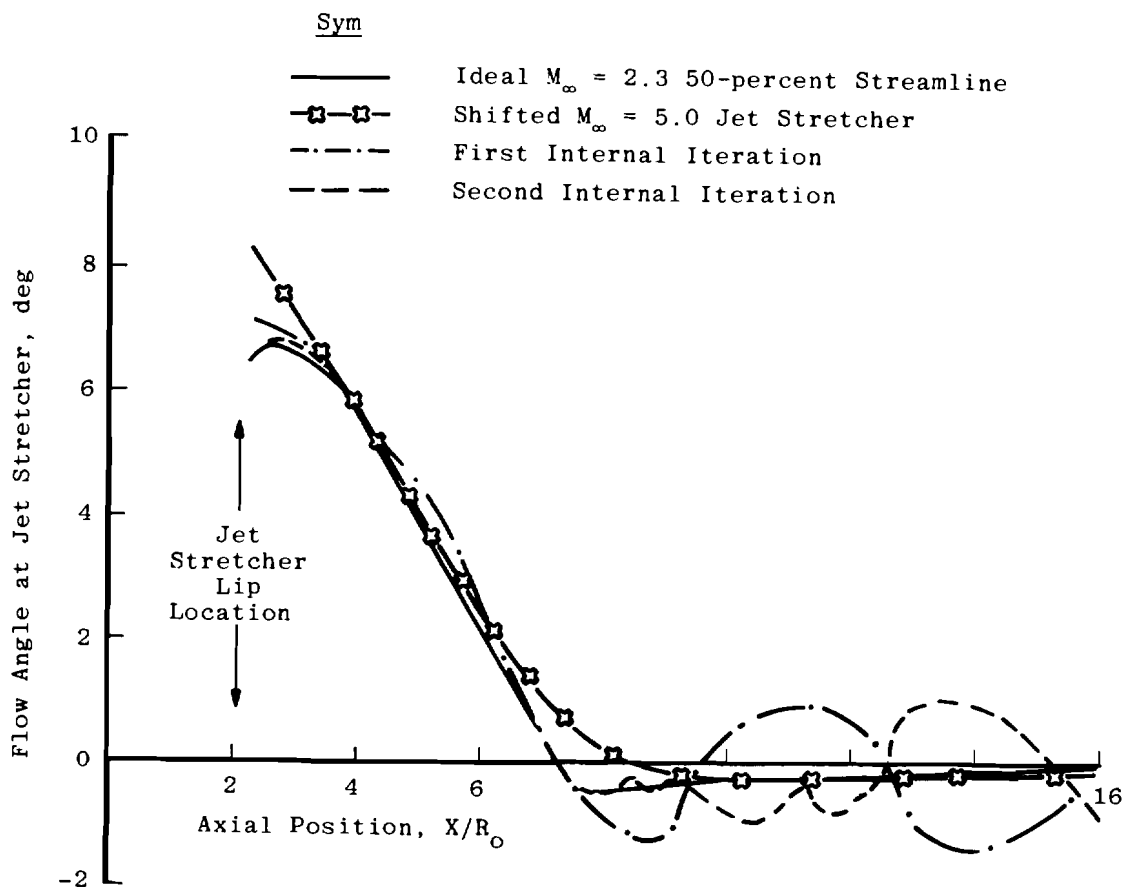


b. Local Mach number, static pressure and flow angle upstream of shoulder

Figure 20. Continued.



c. Local Mach number, static pressure, and flow angle downstream of shoulder
Figure 20. Continued.



d. Comparison of flow angles at jet stretcher
Figure 20. Concluded.

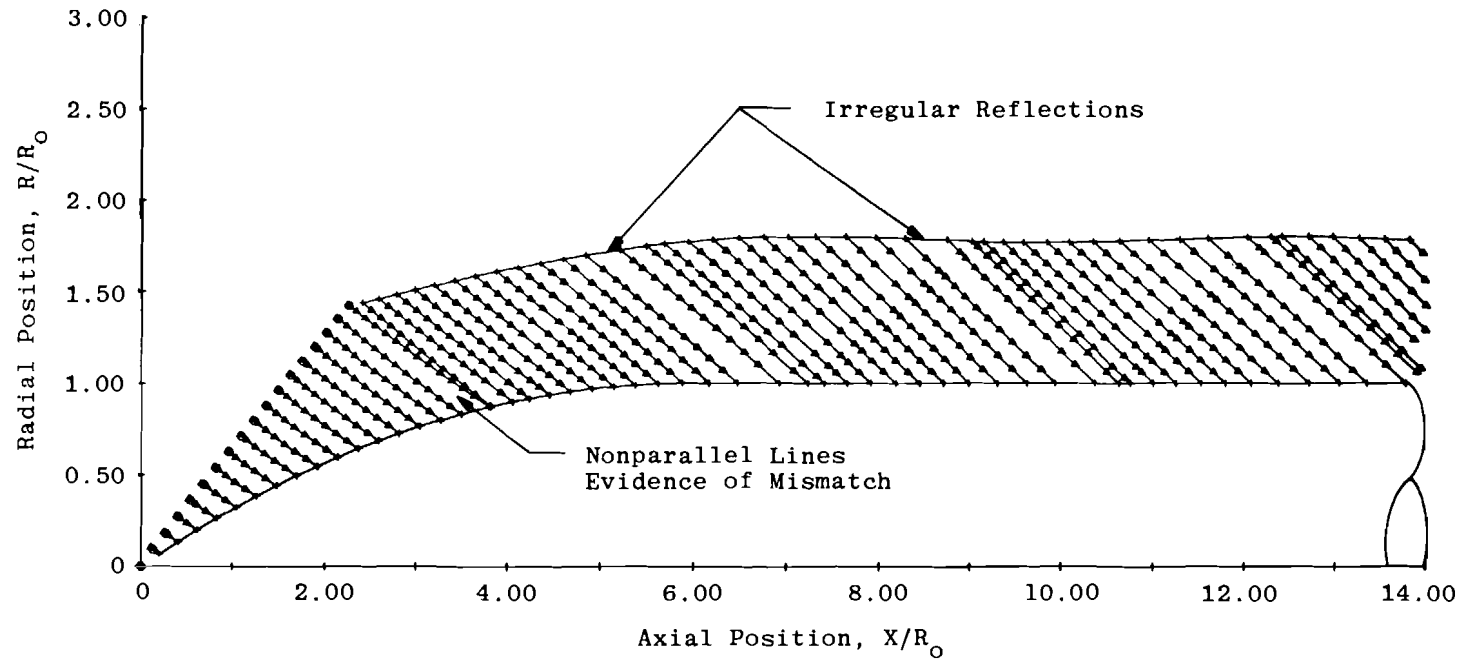


Figure 21. Characteristics lines for second internal iteration.

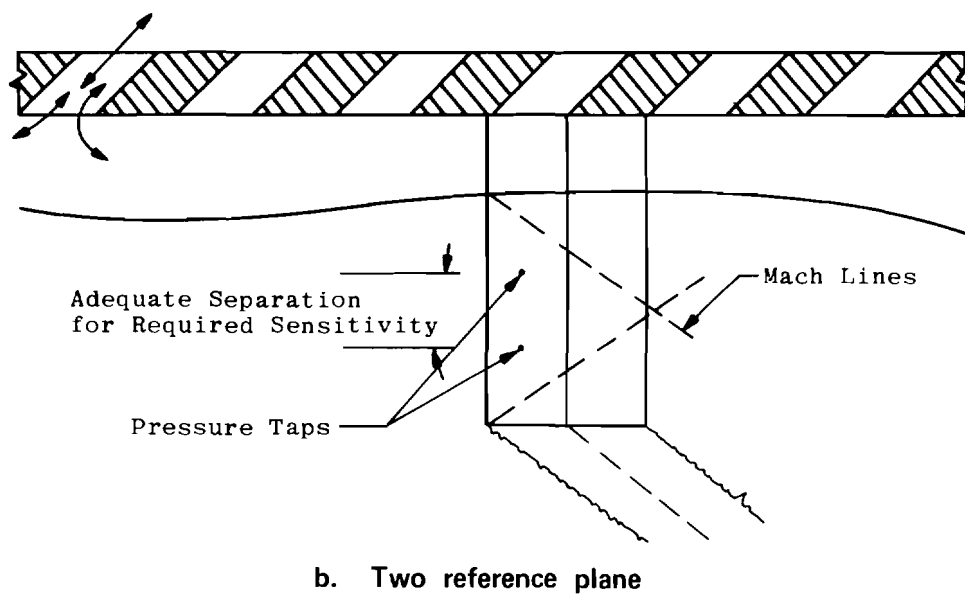
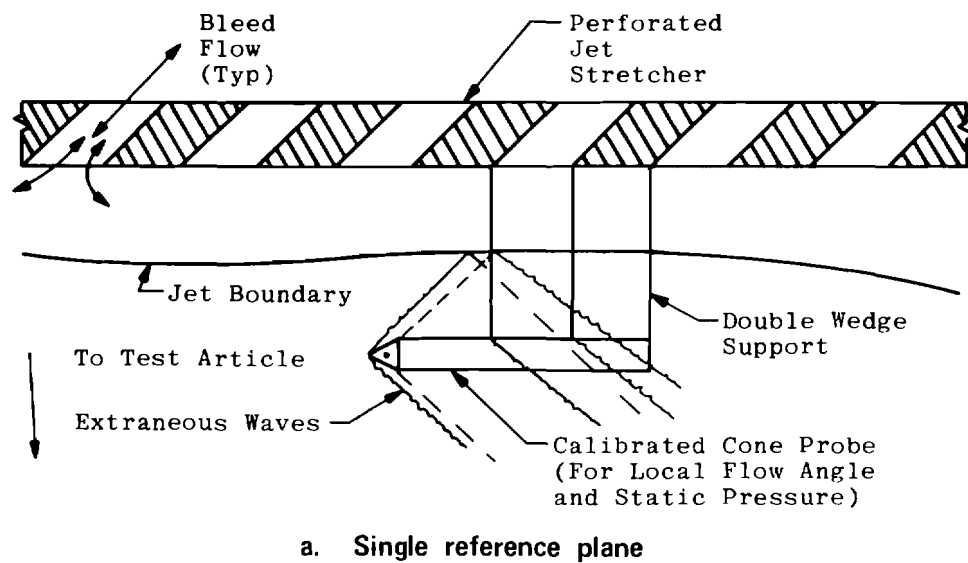


Figure 22. Preliminary thoughts on possible probe-type sensors for perforated adaptable supersonic jet stretchers.

Table 1. Current Free-Jet Design Goals

OPERATIONAL CAPABILITY

Mach Number Range	0.2 \rightarrow 0.8 ⁺ 1.5 \rightarrow 2.5 ⁺
Minimum Attitude Variation Pitch Yaw	-10 deg \rightarrow 25 deg ± 10 deg

NOZZLE FLOW QUALITY

Parameter	Subsonic	Supersonic
Mach Number Variation	± 0.05	± 0.05
Flow Angle Variation	± 1 deg for Pitch ≤ 10 deg ± 1 percent of Pitch Angle for Pitch > 10 deg	± 0.6 deg

APPENDIX A

CONVERGENCE OF THE ADAPTABLE JET STRETCHER IN SUPERSONIC FLOW

To investigate the iteration procedure for the adaptable jet stretcher in supersonic flow, an analytical simulation of a jet stretcher flow field is used to establish conditions for convergence to unconfined flow for supersonic, axisymmetric flow with arbitrary initial conditions. By this simulation, it then becomes possible to ascertain the rate of convergence and establish criteria to reduce significantly the number of iterations required to achieve conditions representative of unconfined flow. The analysis is performed by using a simplified model of the flow within a jet stretcher to examine critically the fundamental theoretical validity of the adaptable jet stretcher concept. It should be emphasized that the analytical simulation presented here differs from the actual test process in the following respect. The power of the actual experimental adaptable jet stretcher installation is that it never requires the calculation of the interior flow (which is presumably complicated, viscous, and shock infested) between the model and the jet stretcher. Only the flow exterior to the jet stretcher (presumed to be inviscid and with only small disturbances) must be determined computationally in the actual test installation.

To provide an analytical proof of convergence of the adaptable jet stretcher concept, an axisymmetric model in supersonic flow will be used. Consequently, the measuring plane, S , consists of a cylinder of radius, R_S . The flow field can be described by the linearized small disturbance equation

$$-B^2 \phi_{xx} + \phi_{rr} - \frac{1}{r} \phi_r = 0 \quad (\text{A-1})$$

where $B^2 = M^2 - 1$, ϕ is the perturbation potential, x is the axial coordinate, and r the radial coordinate. For a body of revolution with a radius distribution $R(x)$, the boundary conditions for unconfined flow are

$$\lim_{r \rightarrow 0} \left(r \frac{\partial \phi}{\partial r} \right) = R(x) - \frac{d R(x)}{d x} = \frac{1}{2\pi} S'(x) \quad (\text{A-2})$$

$$\phi \text{ bounded as } x^2 + r^2 \rightarrow \infty \quad (\text{A-3})$$

where $S(x) = 2\pi R(x)^2$ is the cross-sectional area of the body. Equation (A-3) is equivalent to requiring no incoming waves from infinity. The boundary value problem can be solved using the Heaviside operational transform

$$\bar{g}(p) = p \int_0^\infty g(x) e^{-px} dx \quad (\text{A-4})$$

with the inverse

$$g(x) = \frac{1}{2\pi i} \int_L \bar{g}(p) e^{px} \frac{dp}{p} \quad (A-5)$$

where L is any contour from $A - i\infty$ to $A + i\infty$, A is some finite real constant such that $R(p) > A$, and L passes to the right of all singularities of the integrand. The solution for Eqs. (A-1), (A-2), and (A-3) in the transformed plane is

$$\bar{\phi}(p, r) = \frac{-\bar{S}'(p)}{2\pi} K_0(pBr) \quad (A-6)$$

where K_0 is the modified Bessel function. The corresponding velocity component in the axial direction at the radius R_s is

$$\bar{u}_\infty(p, R_s) = -p \frac{\bar{S}'(p)}{2\pi} K_0(pBR_s) \quad (A-7)$$

$\bar{U}_\infty(p, R_s)$ is therefore the reference value for unconfined flow at the reference surface R_s . Equation (A-6) can be inverted to the physical plane to yield

$$\phi(x, r) = \frac{-1}{2\pi} \int_0^{x-Br} \frac{S'(\zeta)}{\sqrt{(x-\zeta)^2 - B^2 r^2}} d\zeta \quad (A-8)$$

Equation (A-8) is the classical solution for supersonic flow over a slender body of revolution.

If the same axisymmetric body is placed in an axisymmetric jet stretcher, it is presumed that at the reference surface S , interior to the jet stretcher, the pressure distribution is known. In practice, two flow quantities are measured at S ; hence, in a simulation of the interior flow, it is consistent to assume knowledge of a flow variable. However, in the simulation it is necessary to calculate the interior flow to find the second flow variable at S . Again it is emphasized that in a practical application the calculation of the interior flow is unnecessary. The boundary value problem for the interior region is shown in Fig. A-1. The resulting solution for the internal flow in the transformed plane is

$$\bar{\phi}_I(p, r) = \frac{-\bar{S}'(p)}{2\pi} K_0(pBr) + \left[\frac{\bar{G}(p)}{p} + \frac{\bar{S}'(p)}{2\pi} K_0(pBR_s) \right] \frac{I_0(pBr)}{I_0(pBR_s)} \quad (A-9)$$

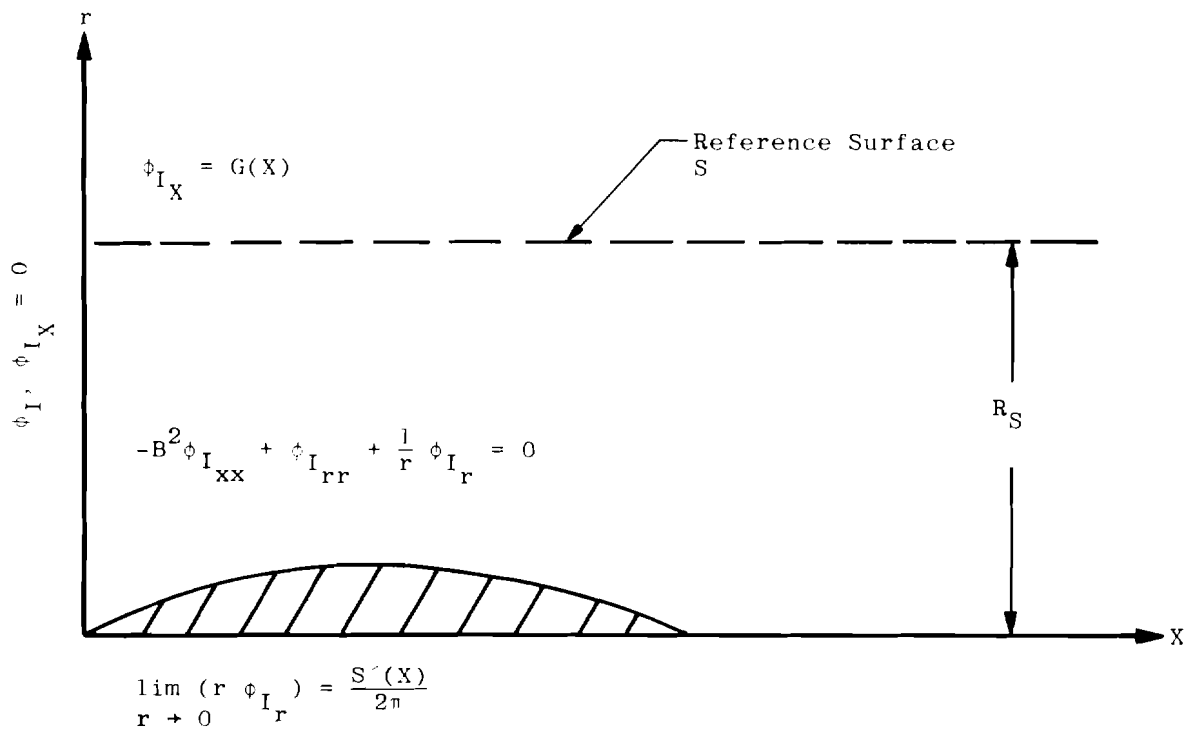


Figure A-1. Boundary value problem for the interior region.

where $\bar{G}(p)$ is the transformed known pressure distribution at the surface S, i.e.,

$$G(X) = \left. \frac{\partial \phi_I}{\partial X} \right|_{r=R_s} = u_I(X, R_s) = -\frac{1}{2} C_p(X, R_s) \quad (\text{A-10})$$

where $C_p = (p - p_\infty)/q_\infty$ is the pressure coefficient.

Consequently, the normal velocity (i.e., the second flow variable) at the control surface is

$$\begin{aligned} \bar{v}_I(p, R_s) &= \left. \frac{\partial \bar{\phi}_I}{\partial r} \right|_{r=R_s} = pB \frac{\bar{S}'(p)}{2\pi} K_1(pBR_s) \\ &+ pB \left[\frac{\bar{G}(p)}{p} + \frac{\bar{S}'(p)}{2\pi} K_0(pBR_s) \right] \frac{I_1(pBR_s)}{I_0(pBR_s)} \end{aligned} \quad (\text{A-11})$$

The next step in the adaptable jet stretcher concept is to use one of the measured flow variables at S to determine the unique functional relationship with the other flow variable under conditions of unconfined flow at infinity. If $v_E(X, R_s) = v_I(X, R_s)$ is the flow variable chosen at the reference surface S, then the exterior region boundary value problem is that shown in Fig. A-2.

The corresponding solution for the exterior region, in transformed variables, is

$$\bar{\phi}_E(p, r) = - \frac{\bar{v}_I(p, R_s) K_0(pBr)}{pBK_1(pBR_s)} \quad (\text{A-12})$$

Substitution of Eq. (A-11) yields

$$\begin{aligned} \bar{\phi}_E(p, r) &= - \frac{1}{pB} \left\{ \frac{\bar{S}'(p)}{2\pi} pB \left[K_1(\alpha) \right. \right. \\ &\left. \left. + \frac{I_1(\alpha)}{I_0(\alpha)} K_0(\alpha) \right] + B\bar{G}(p) \frac{I_1(\alpha)}{I_0(\alpha)} \right\} \frac{K_0(pBr)}{K_1(\alpha)} \end{aligned} \quad (\text{A-13})$$

where $\alpha = pBR_s$. Consequently, the exterior value of the axial velocity at the reference surface is

$$\bar{u}_E(p, R_s) = - \left\{ \frac{\bar{S}'(p) p}{2\pi} \left[K_1(\alpha) + \frac{I_1(\alpha)}{I_0(\alpha)} K_0(\alpha) \right] + \bar{G}(p) \frac{I_1(\alpha)}{I_0(\alpha)} \right\} \frac{K_0(\alpha)}{K_1(\alpha)} \quad (\text{A-14})$$

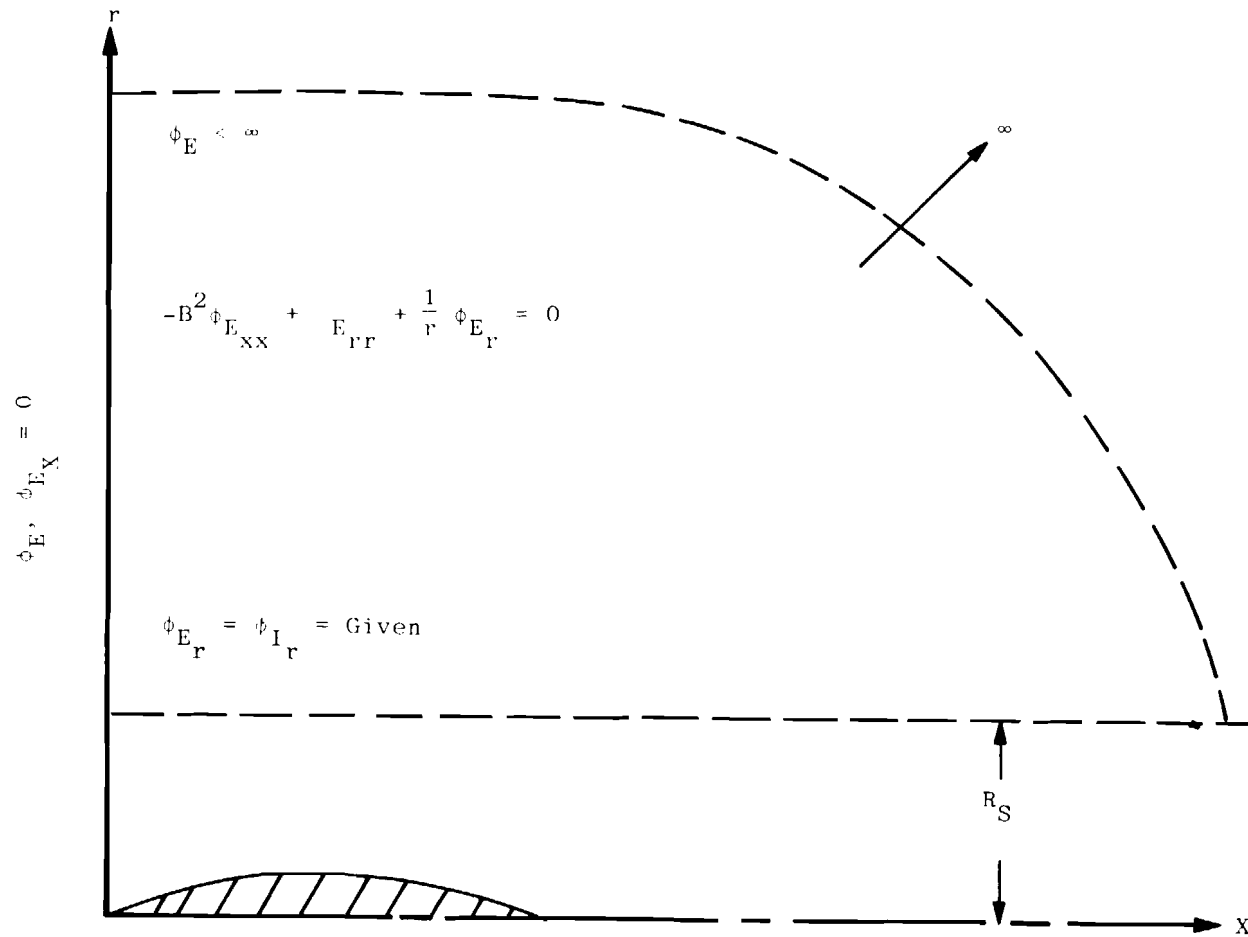


Figure A-2. Boundary value problem for the exterior unconfined flow regions.

The convergence of the iteration procedure will be demonstrated in the transformed plane, since the functional relationships are in simple algebraic form in that plane. The iteration is initiated with an arbitrary distribution of $\bar{u}_l^{(0)} = \bar{G}^{(0)}$ at $r = R_s$. Following the iteration scheme shown in Fig. 4, the n th iterative value for \bar{u}_l at R_s can be obtained by using Eqs. (A-11) and (A-13) appropriately

$$\begin{aligned}\bar{u}_l^{(n)}(p, R_s) &= \omega \bar{u}_l^{(n-1)}(p, R_s) + (1 - \omega) \bar{u}_l^{(n-1)}(p, R_s) \\ &= \Omega^n \bar{G}^{(0)} + \Lambda \frac{(1 - \Omega^n)}{(1 - \Omega)}\end{aligned}\quad (A-15)$$

where

$$\Omega = (1 - \omega) - \omega \frac{I_1(\alpha) K_0(\alpha)}{I_0(\alpha) K_1(\alpha)} \quad (A-16)$$

$$\Lambda = \frac{\bar{S}'(p)}{2\pi} \omega \left[-p \frac{K_0(\alpha)}{K_1(\alpha)} \left(K_1(\alpha) + \frac{K_0(\alpha) I_1(\alpha)}{I_0(\alpha)} \right) \right] \quad (A-17)$$

and where ω is a relaxation parameter introduced to accelerate convergence of the iterative procedure. It should be noted that since p is a complex variable, then Ω , Λ , and ω are in general also complex variables. As long as $|\Omega| < 1$ is required, then it can be asserted that as $n \rightarrow \infty$, then $\Omega^n \rightarrow 0$, hence

$$\begin{aligned}\lim_{n \rightarrow \infty} \bar{u}_l^{(n)}(p, R_s) &= \frac{\Lambda}{1 - \Omega} \\ &= - \frac{\bar{S}'(p)}{2\pi} p K_0(pBR_s) \\ &= \bar{u}_\infty(p, R_s)\end{aligned}\quad (A-18)$$

by comparison with Eq. (A-7). Hence, convergence of the adaptable jet stretcher concept to unconfined flow is established independent of the initial condition, $\bar{G}^{(0)}$, for axisymmetric supersonic flow. For $|\Omega| < 1$ requires

$$\left| 1 - \omega - \omega \frac{I_1(\alpha)}{I_0(\alpha)} \frac{K_0(\alpha)}{K_1(\alpha)} \right| < 1$$

or

$$0 < \omega < \frac{2}{1 + \frac{I_1(\alpha)}{I_0(\alpha)} \frac{K_0(\alpha)}{K_1(\alpha)}} \quad (A-19)$$

within this range it may be possible to select a value of ω such that convergence to unconfined flow can be reduced to a finite number of iterations. From Eq. (A-15) it is obvious that the effect of the initial configuration, $\bar{G}^{(0)}$, would be diminished the closer the magnitude of Ω is to zero. If $\Omega = 0$, a value for ω can be determined, namely,

$$\omega = \alpha I_0(\alpha) K_1(\alpha) \quad (\text{A-20})$$

To see the effect of this value of the relaxation factor on convergence of the method, Eq. (A-20) is substituted into Eq. (A-15) for the case $n = 1$, i.e., the first iteration,

$$\begin{aligned} \bar{u}_1^{(1)}(p, R_s) &= \Lambda = \alpha I_0(\alpha) K_1(\alpha) \frac{\bar{S}'(p)}{2\pi} \left[-p \frac{K_0(\alpha)}{K_1(\alpha)} \left(K_1(\alpha) + \frac{K_0(\alpha) I_1(\alpha)}{I_0(\alpha)} \right) \right] \\ &= \frac{-\bar{S}'(p)}{2\pi} p K_0(pBR_s) = \bar{u}_\infty(p, R_s) \end{aligned} \quad (\text{A-21})$$

The value of ω in Eq. (A-20) is an optimum relaxation factor in that it produces unconfined flow in a single adjustment of the adaptable jet stretcher.

In principle then, knowing the two velocity components, $u_1^{(0)}(X, R_s)$ and $v_1^{(0)}(X, R_s)$, is sufficient to determine directly the requirements for unconfined flow. Combining Eqs. (A-12), (A-15), and (A-20), it can be shown that

$$\begin{aligned} \bar{u}_\infty(p, R_s) &= \bar{u}_1^{(1)}(p, R_s) \\ &= \omega \left[\frac{-\bar{v}_1^{(0)}(p, R_s)}{B} \frac{K_0(\alpha)}{K_1(\alpha)} - \bar{u}_1^{(0)}(p, R_s) \right] - \bar{u}_1^{(0)}(p, R_s) \\ &= \alpha I_1(\alpha) K_0(\alpha) \bar{u}_1^{(0)}(p, R_s) - \frac{\alpha K_0(\alpha) I_0(\alpha)}{B} \bar{v}_1^{(0)}(p, R_s) \end{aligned} \quad (\text{A-22})$$

Using the convolution theorem for Heaviside transforms, Eq. (A-22) can be inverted to the physical plane to yield

$$u_\infty(X, R_s) = \int_0^\infty u_1^{(0)}(\zeta, R_s) H^{-1}(F_1) d\zeta - \int_0^\infty \frac{v_1^{(0)}(\zeta, R_s)}{B} H^{-1}(F_2) d\zeta \quad (\text{A-23})$$

where the H^{-1} are the inverse Heaviside transforms

$$H^{-1}(F_1) = \frac{1}{2\pi i} \int_{A-i\infty}^{A+i\infty} p^2 BR_s I_1(pBR_s) K_0(pBR_s) e^{p(x-\zeta)} \frac{dp}{p} \quad (\text{A-24})$$

$$H^{-1}(F_2) = \frac{1}{2\pi i} \int_{A-i\infty}^{A+i\infty} p I_0(pBR_s) K_0(pBR_s) e^{p(x-\zeta)} \frac{dp}{p} \quad (\text{A-25})$$

In principle, Eqs. (A-24) and (A-25) can be inverted either analytically or numerically. Hence, Eq. (A-23) verifies that if $u_1^{(0)}(X, R_s)$ and $v_1^{(0)}(X, R_s)$ are known from measurements at the control surface, the conditions for unconfined flow can be determined directly without recourse to mathematical modeling of the test article or jet stretcher configuration.

In a similar manner it is possible to show that

$$\bar{v}_\infty(p, R_s) = -\alpha B K_1(\alpha) I_1(\alpha) \bar{u}_1^{(0)}(p, R_s) + \alpha K_1(\alpha) I_0(\alpha) \bar{v}_1^{(0)}(p, R_s) \quad (A-26)$$

which can be inverted to the physical plane in the same manner as Eq. (A-22).

NOMENCLATURE

C_p	Pressure coefficient ($C_p = P - P_\infty / q_\infty$)
D	Diameter
k	Weighting factor
L_o	Length of forebody to shoulder
M	Mach number
P	Static pressure
q	Dynamic pressure
R	Radius
R_B	Local body radius
R_C	Radius of curvature
Re_∞	Free flight or reference Reynolds number
R_o	Aft body radius (nondimensionalizing parameter for all geometric details)
S	Reference surface
X	Axial position
Θ	Flow angle (positive, away from body axis)

SUBSCRIPTS

E	Exterior region
I	Interior region
JB	Jet boundary
NE	Nozzle exit or duct
US	Undisturbed upstream streamline
∞	Free flight or reference conditions

SUPERSCRIPTS

0,1,2	Computational iteration number
-------	--------------------------------

COMPUTER PROGRAM ABBREVIATIONS

A3DMOC	Armstrong three-dimensional method of characteristics (Ref. 12)
CNAP	Cline nozzle and plume inviscid finite difference (Ref. 13)
D-N	Douglas-Neumann panel method potential flow (Ref. 15)
LMOC	Lockheed method of characteristics (Ref. 11)
S-J	South-Jameson finite-difference, infinite stream, full potential relaxation (Ref. 10)
W-M	Wehofer-Moger inviscid, finite-difference, time-dependent conservation (Ref. 14)